Supporting Information

for

Assessing the effect of substituents in ferrocene acylphosphines and their impact on gold-catalysed reactions

Petr Vosáhlo and Petr Štěpnička*

Contents

X-ray crystallography

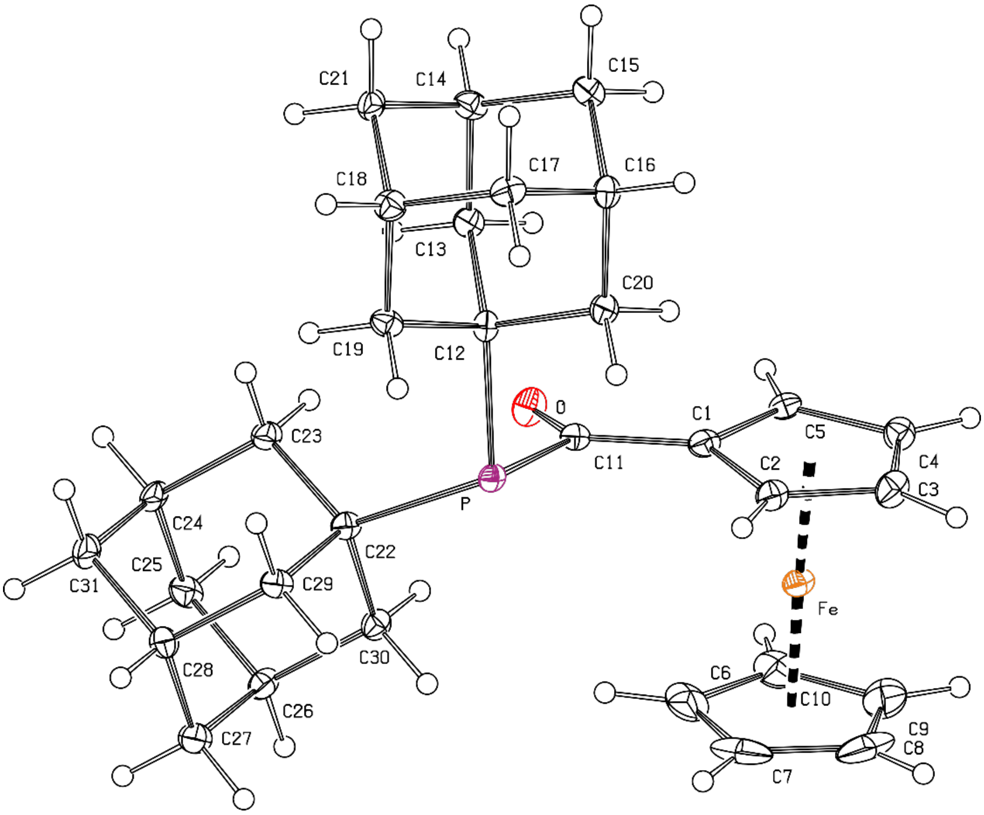

Figure S1 PLATON plot of the molecular structure of **1c** (30% probability ellipsoids)

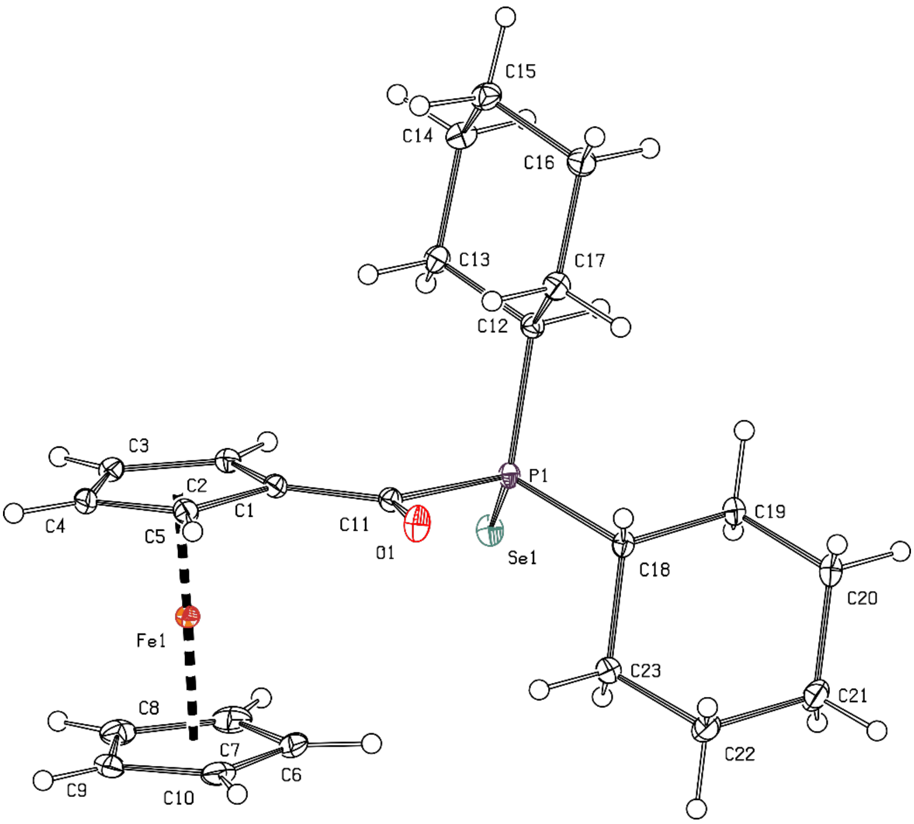

Figure S2 PLATON plot of the molecular structure of **2b** (30% probability ellipsoids)

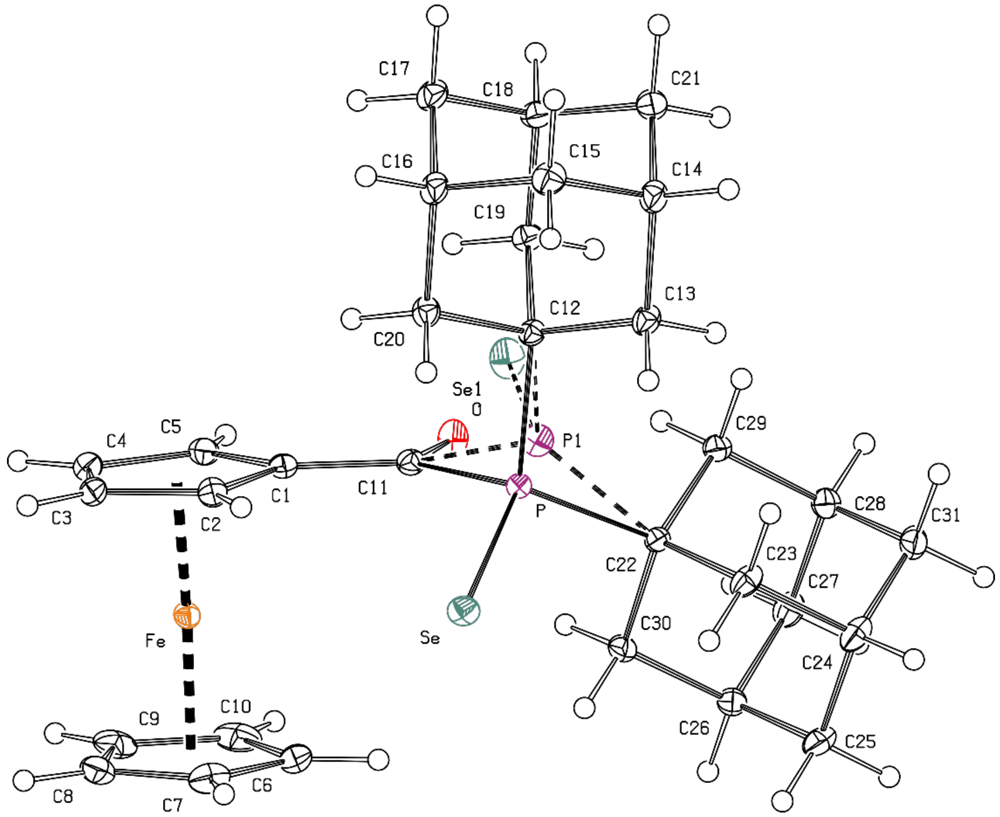

Figure S3 PLATON plot of the molecular structure of **2c** (30% probability ellipsoids; both positions of the disordered P=Se moiety are shown)

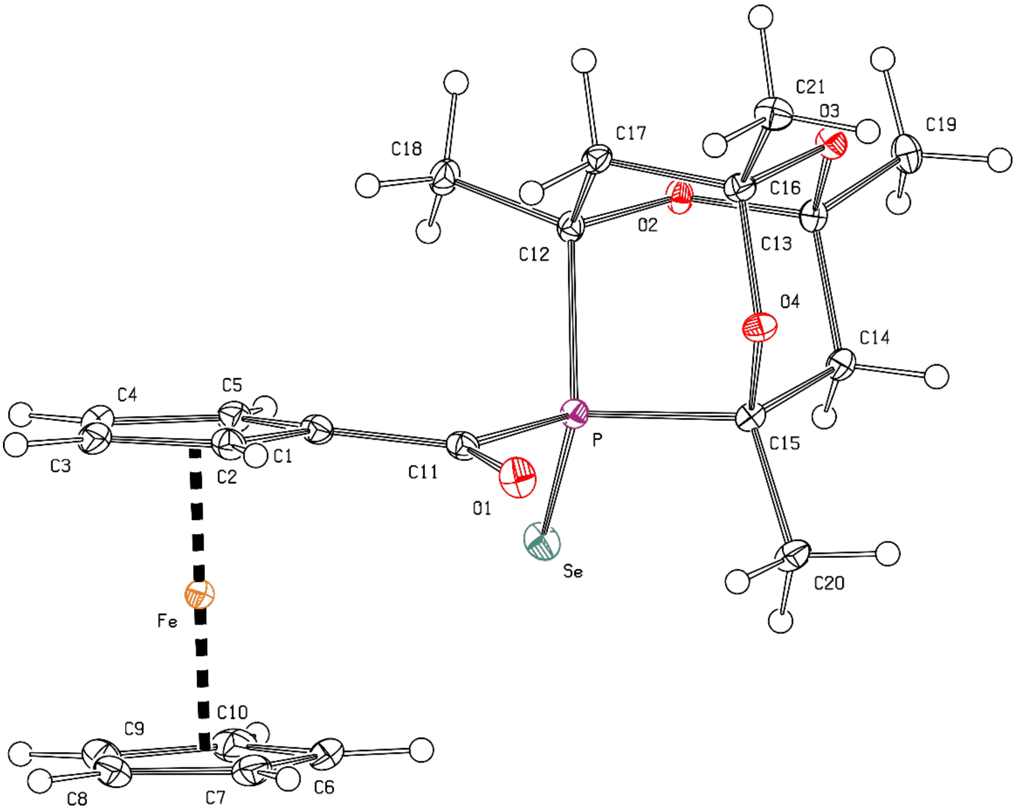

Figure S4 PLATON plot of the molecular structure of **2d** (30% probability ellipsoids)

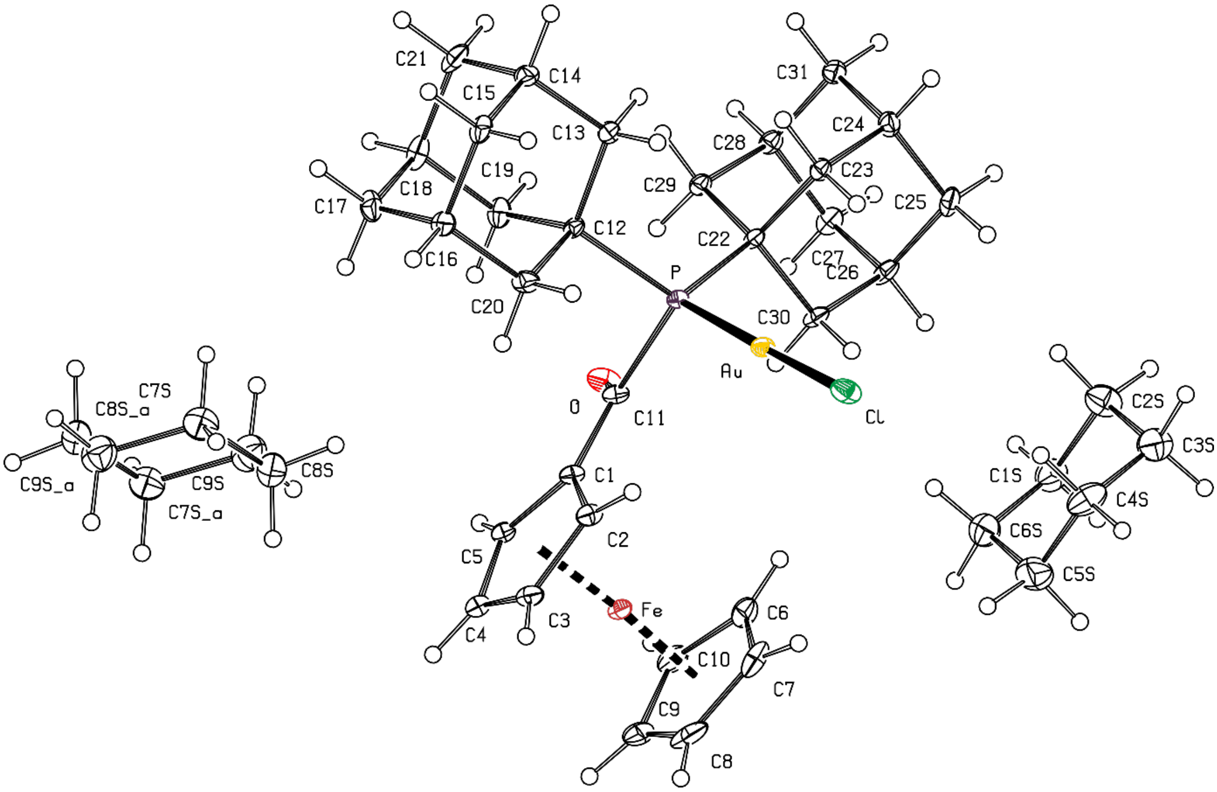

Figure S5 PLATON plot of the molecular structure of **3c**·1.5C_6H_{12} (30% probability ellipsoids)

Table S1. Selected crystallographic data and structure refinement parameters.[a]

Compound	**1c**	**2b**	**2c**
Formula	$C_{31}H_{39}FeOP$	$C_{23}H_{31}FeOPSe$	$C_{31}H_{39}FeOPSe$
M	514.44	489.26	593.40
Crystal system	monoclinic	monoclinic	monoclinic
Space group	$P\,2_1/c$ (no. 14)	$P\,2_1/c$ (no. 14)	$P\,2_1/c$ (no. 14)
T [K]	120 (2)	120(2)	120(2)
a [Å]	10.8579(5)	14.2338(3)	13.6384(3)
b [Å]	6.7355(3)	10.1725(2)	11.0185(3)
c [Å]	34.096(2)	15.2719(3)	17.3274(4)
α [°]			
β [°]	98.833(3)	95.577(1)	98.677(1)
γ [°]			
V [Å]^3	2464.0(2)	2200.80(8)	2574.1(1)
Z	4	4	4
μ(Mo Kα) [mm^{-1}]	5.681	2.422	2.086
Diffrns collected	30648	23550	38493
Independent diffrns	5067	5023	5888
Observed[a] diffrns	4821	4799	5643
R_{int}[b] [%]	6.40	1.60	1.98
No. of parameters	308	244	335
R[b] obsd diffrns [%]	6.74	1.69	2.62
R, wR[b] all data [%]	7.19, 17.26	1.79, 4.39	2.74, 5.98
$\Delta\rho$ [e Å^{-3}]	0.527, –1.254	0.339, –0.240	0.751, –0.398

[a] Diffractions with $I > 2\sigma(I)$. [b] Definitions: $R_{int} = \Sigma|F_o^2 - F_o^2(\text{mean})|/\Sigma F_o^2$, where $F_o^2(\text{mean})$ is the average intensity of symmetry-equivalent diffractions. $R = \Sigma||F_o| - |F_c||/\Sigma|F_o|$, $wR = [\Sigma\{w(F_o^2 - F_c^2)^2\}/\Sigma w(F_o^2)^2]^{1/2}$.

Table S1 continued

Compound	**2d**	**3c**·1.5C_6H_{12}
Formula	$C_{21}H_{25}FeO_4PSe$	$C_{31}H_{39}AuClFeOP\cdot1.5C_6H_{12}$
M	507.19	873.09
Crystal system	triclinic	triclinic
Space group	*P* –1 (no. 2)	*P* –1 (no. 2)
T [K]	150(2)	120(2)
a [Å]	7.5245(4)	11.2049(9)
b [Å]	8.1925(4)	12.206(1)
c [Å]	18.405(1)	13.816(1)
α [°]	78.114(2)	82.383(2)
β [°]	82.669(2)	78.024(2)
γ [°]	63.498(2)	76.254(2)
V $[Å]^3$	992.76(9)	1788.5(2)
Z	2	2
μ(Mo Kα) $[mm^{-1}]$	2.699	4.653
Diffrns collected	44878	131798
Independent diffrns	4565	8225
Observed[a] diffrns	4457	7975
R_{int}^b [%]	2.38	5.06
No. of parameters	257	407
R^b obsd diffrns [%]	1.75	2.96
R, wR^b all data [%]	1.80, 4.67	3.06, 9.37
Δρ [e $Å^{-3}$]	0.383, –0.248	1.602, –1.423

Buried volume calculation

Buried volumes (V_{bur}) for individual ligands were calculated using the crystal structure coordinates of selenides **2a-d**, for which a complete series was available. To minimise the influence of ferrocenyl group orientation, which also affects the ligand sterics, the buried volume was determined by a unified approach as follows: the C(O)–P bond was oriented in East-West direction with the ferrocenyl group in the East part and the phosphine substituents in the West section as illustrated in Figure S6. The V_{bur} presented here is an average of V_{bur} estimated in the NW and SW quadrants by SambVca 2.1 web tool (Table S2).[1] The following parameters were used: P–Au distance 2.28 Å, sphere radius 3.50 Å, hydrogen atoms omitted, bond radii scaled by 1.17.

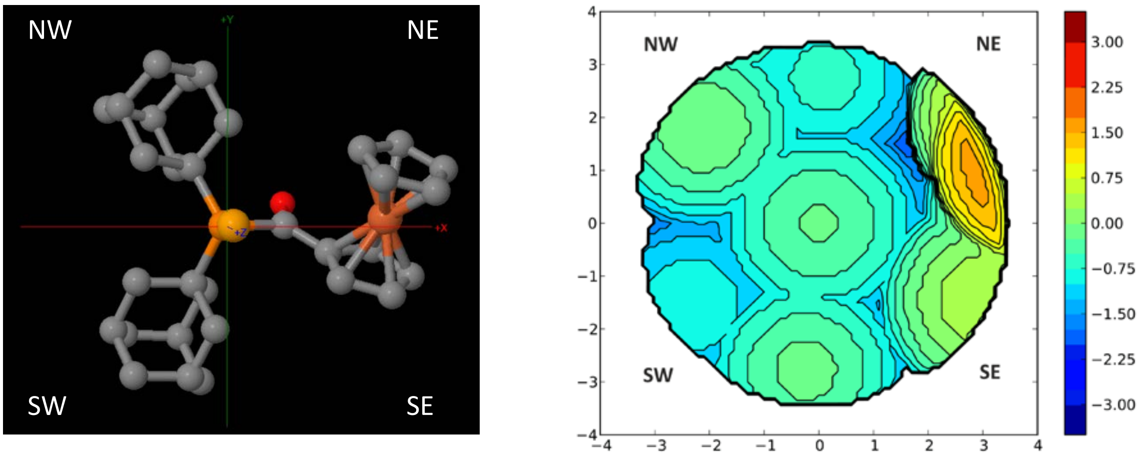

Figure S6 (left) Setting for V_{bur} estimation from the crystal structure data illustrated for compound **2c** and (right) the calculated steric map[2]

Table S2 Partial and average V_{bur} values

Parameter	**2a**	**2b**	**2c**	**2d**
V_{bur}(NW) [%]	31.6	28.5	40.1	30.2
V_{bur}(SW) [%]	36.0	33.7	35.9	30.6
V_{bur}(av.) [%]	**33.8**	**31.1**	**38.0**	**30.4**

Copies of the NMR spectra

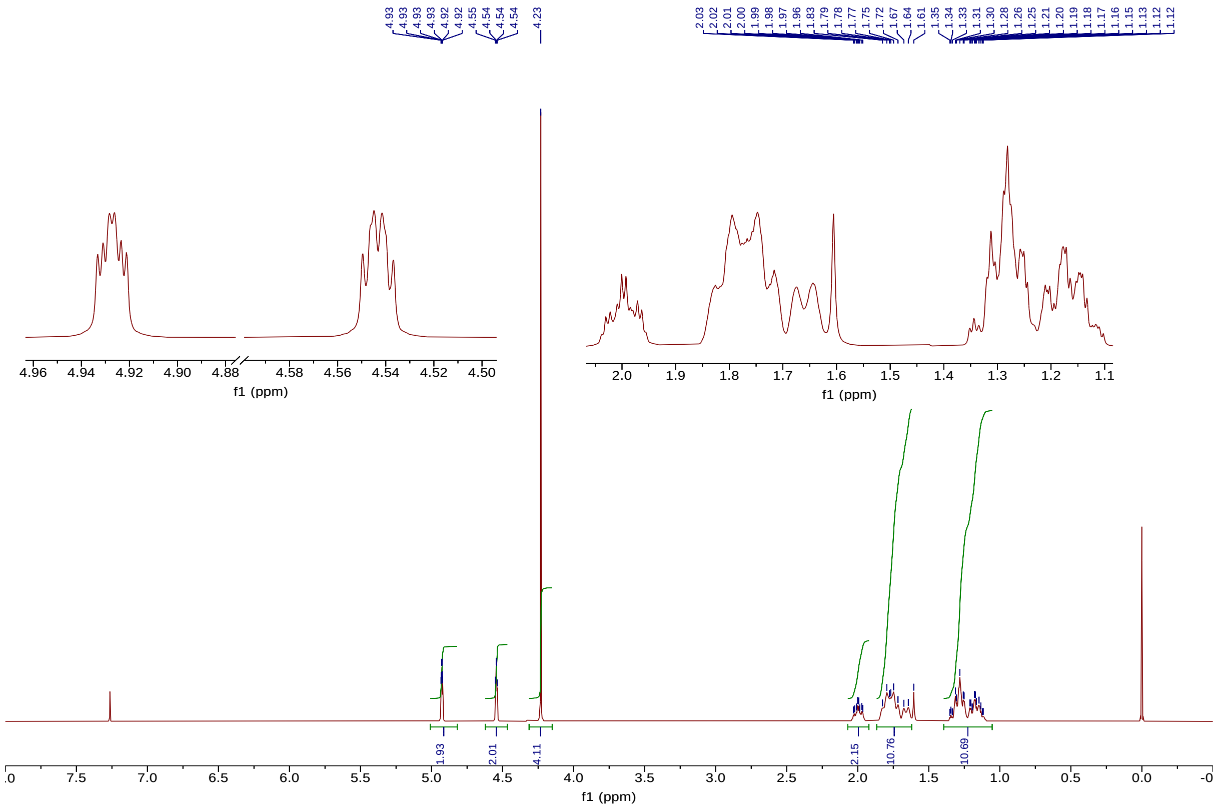

Figure S7 ^{1}H NMR spectrum (400 MHz, $CDCl_3$) of **1b**

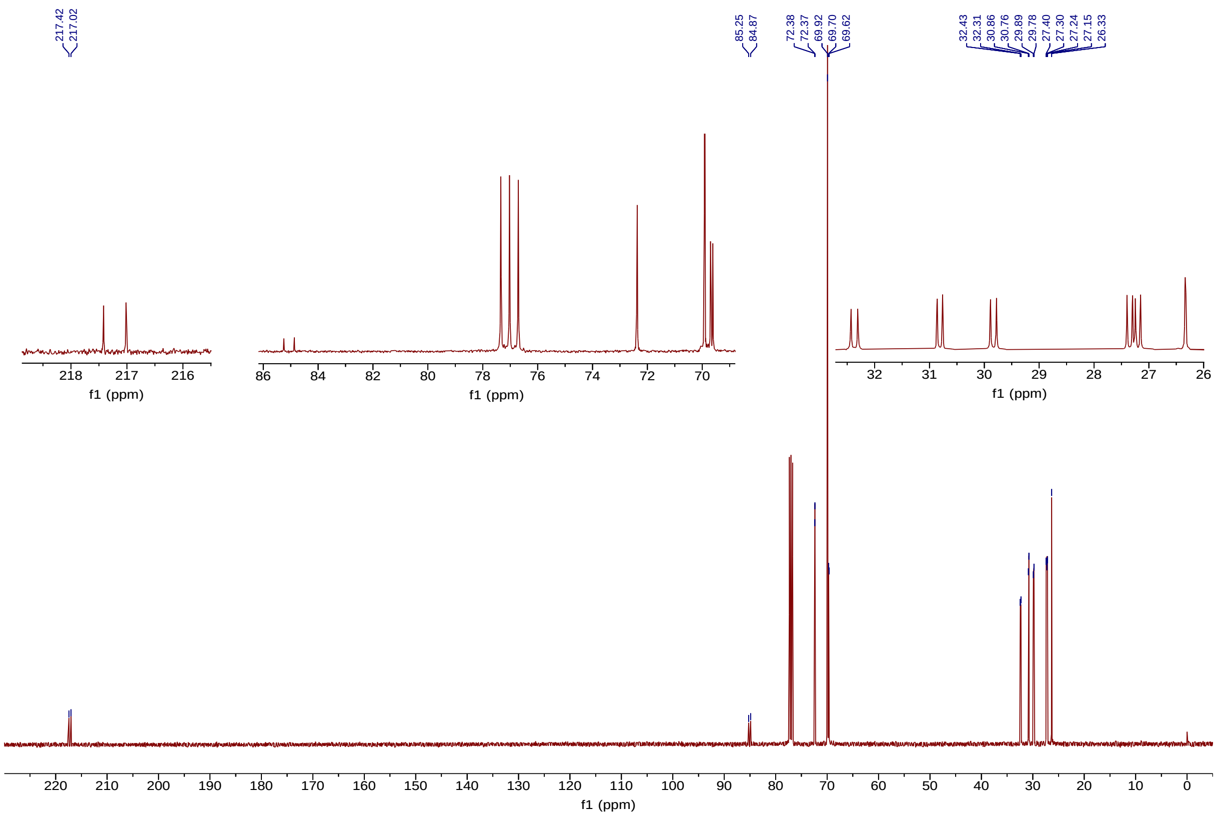

Figure S8 $^{13}C\{^{1}H\}$ NMR spectrum (101 MHz, $CDCl_3$) of **1b**

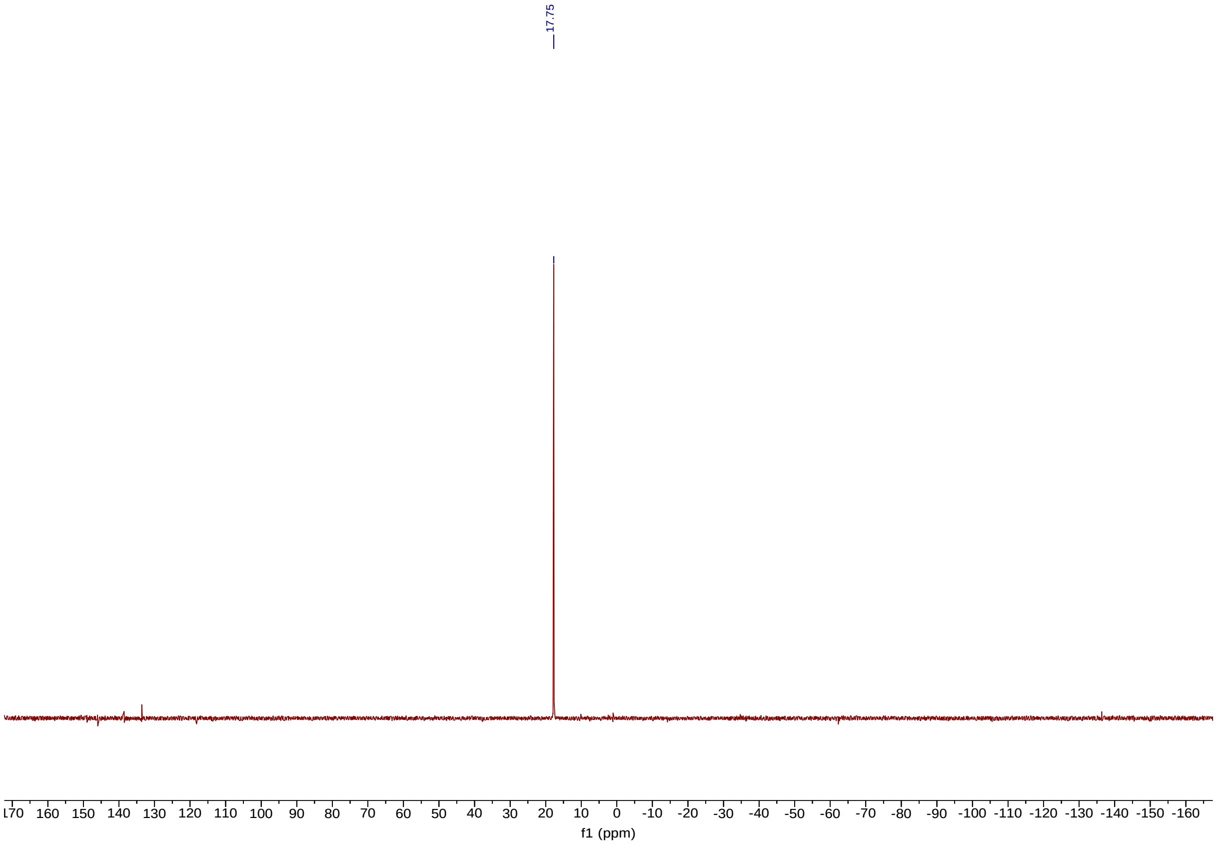

Figure S9 $^{31}P\{^{1}H\}$ NMR spectrum (162 MHz, $CDCl_3$) of **1b**

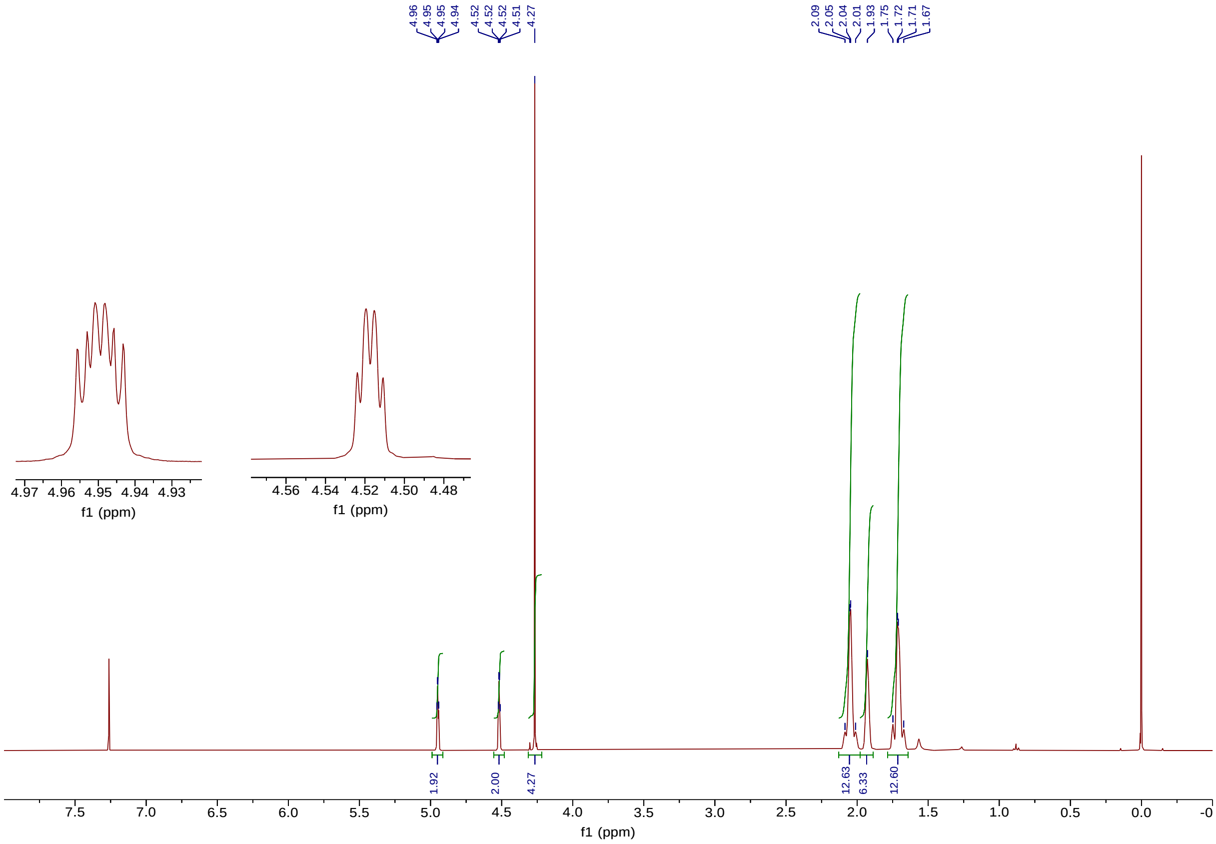

Figure S10 ^{1}H NMR spectrum (400 MHz, $CDCl_3$) of **1c**

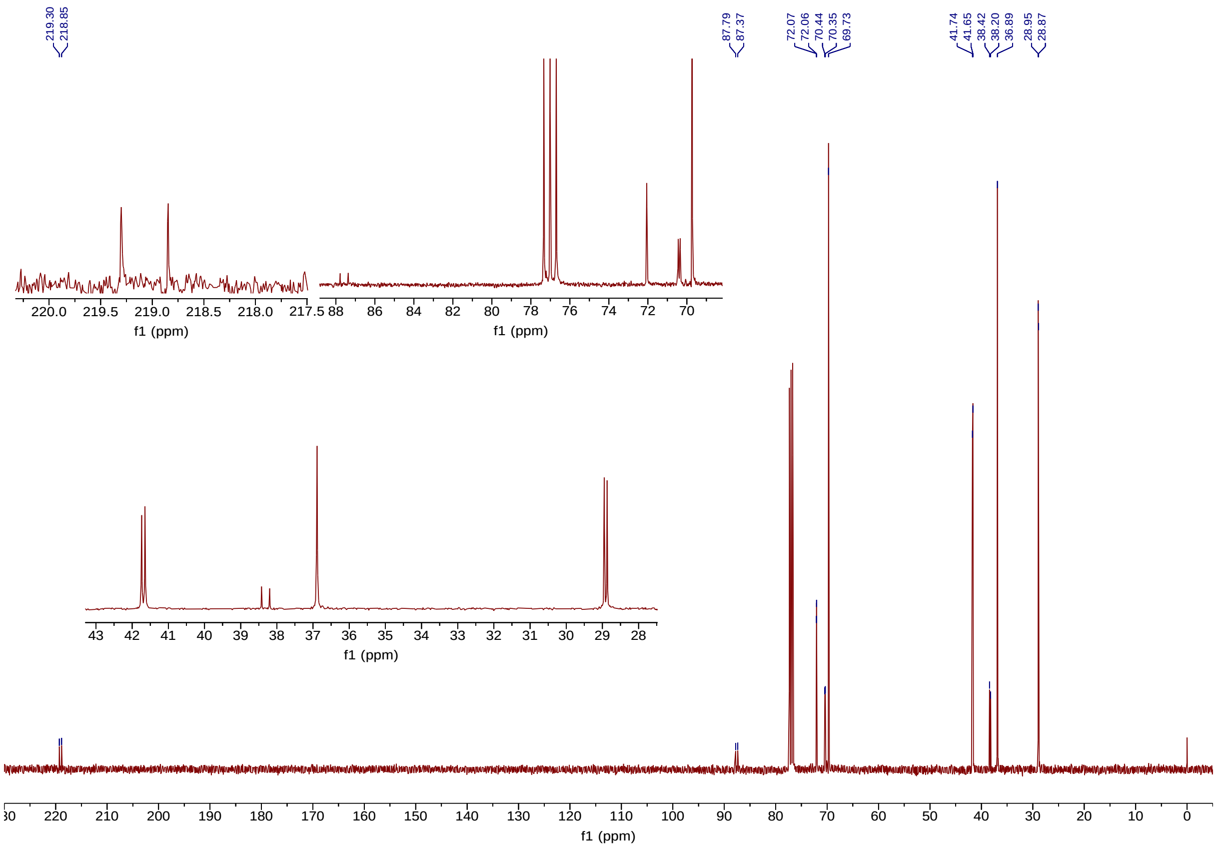

Figure S11 $^{13}C\{^{1}H\}$ NMR spectrum (101 MHz, $CDCl_3$) of **1c**

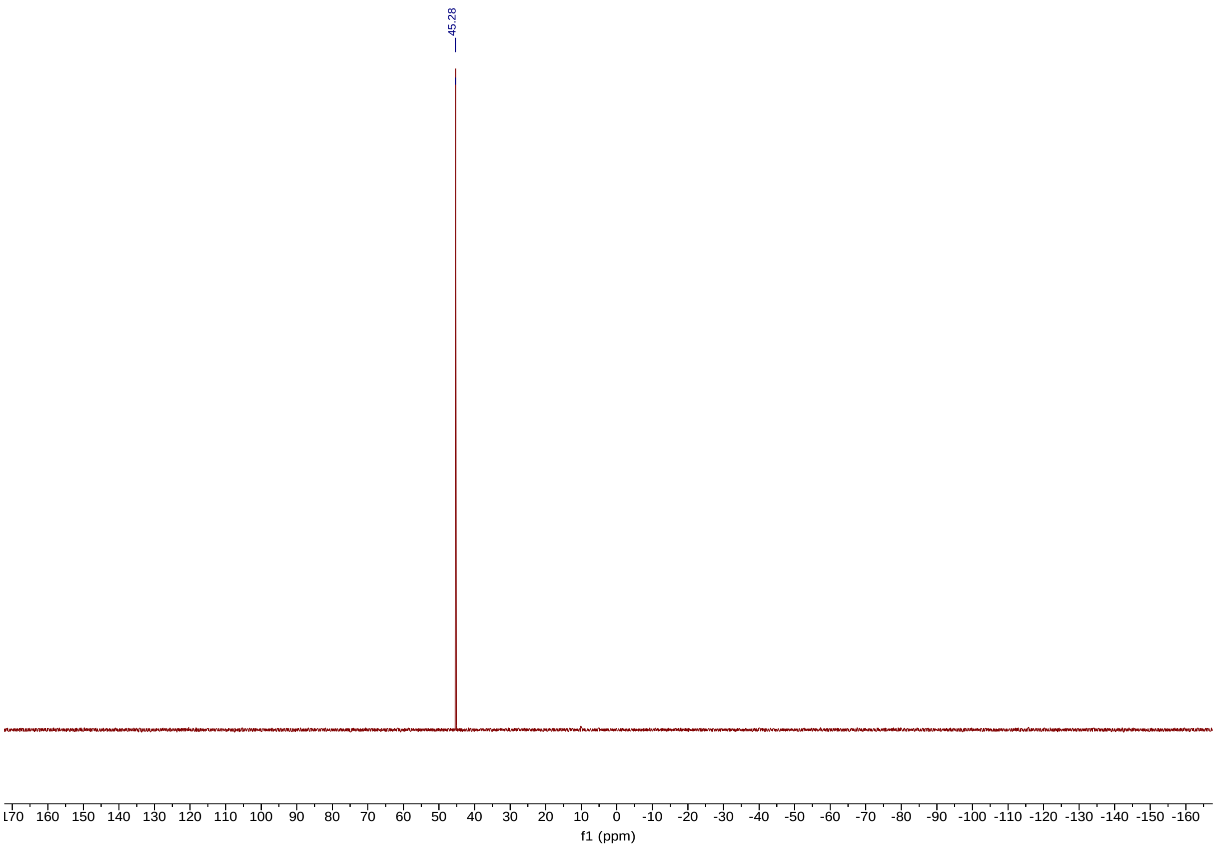

Figure S12 $^{31}P\{^{1}H\}$ NMR spectrum (162 MHz, $CDCl_3$) of **1c**

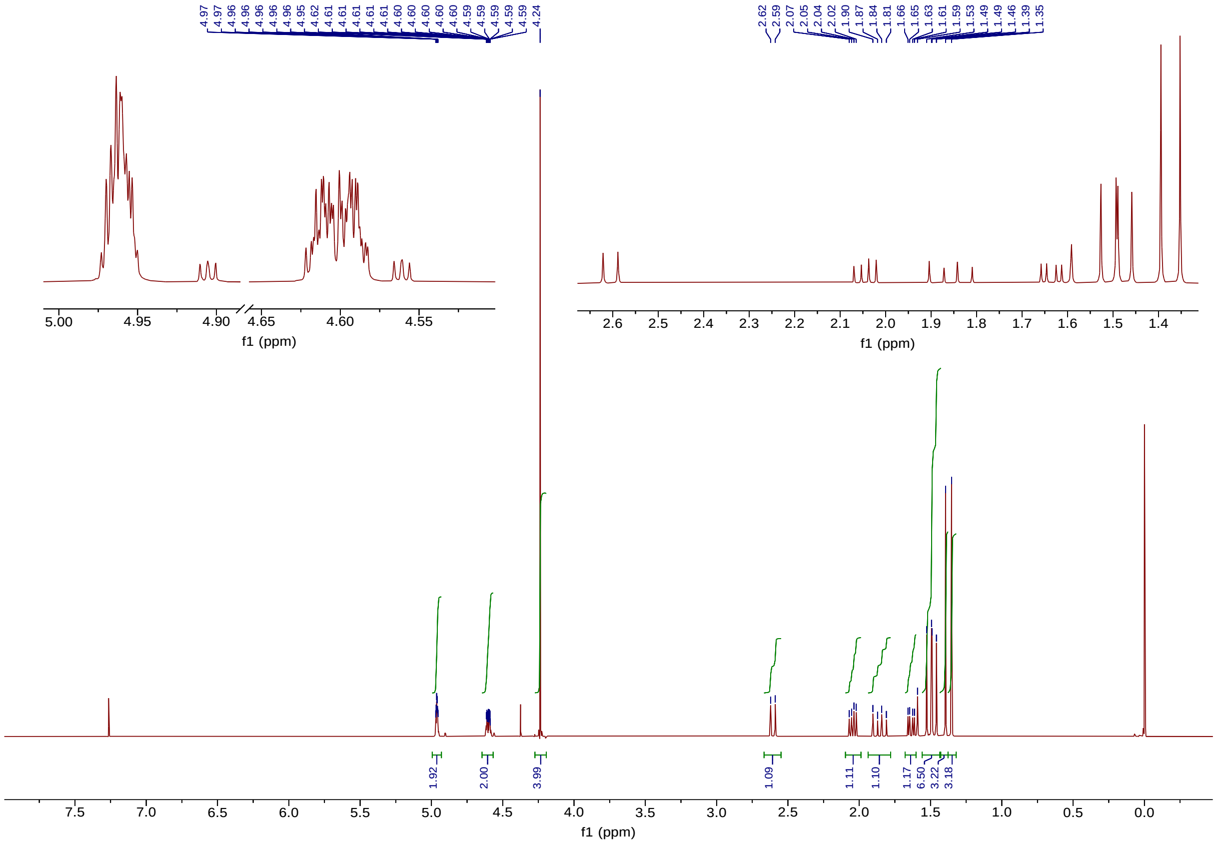

Figure S13 ^{1}H NMR spectrum (400 MHz, $CDCl_3$) of **1d**

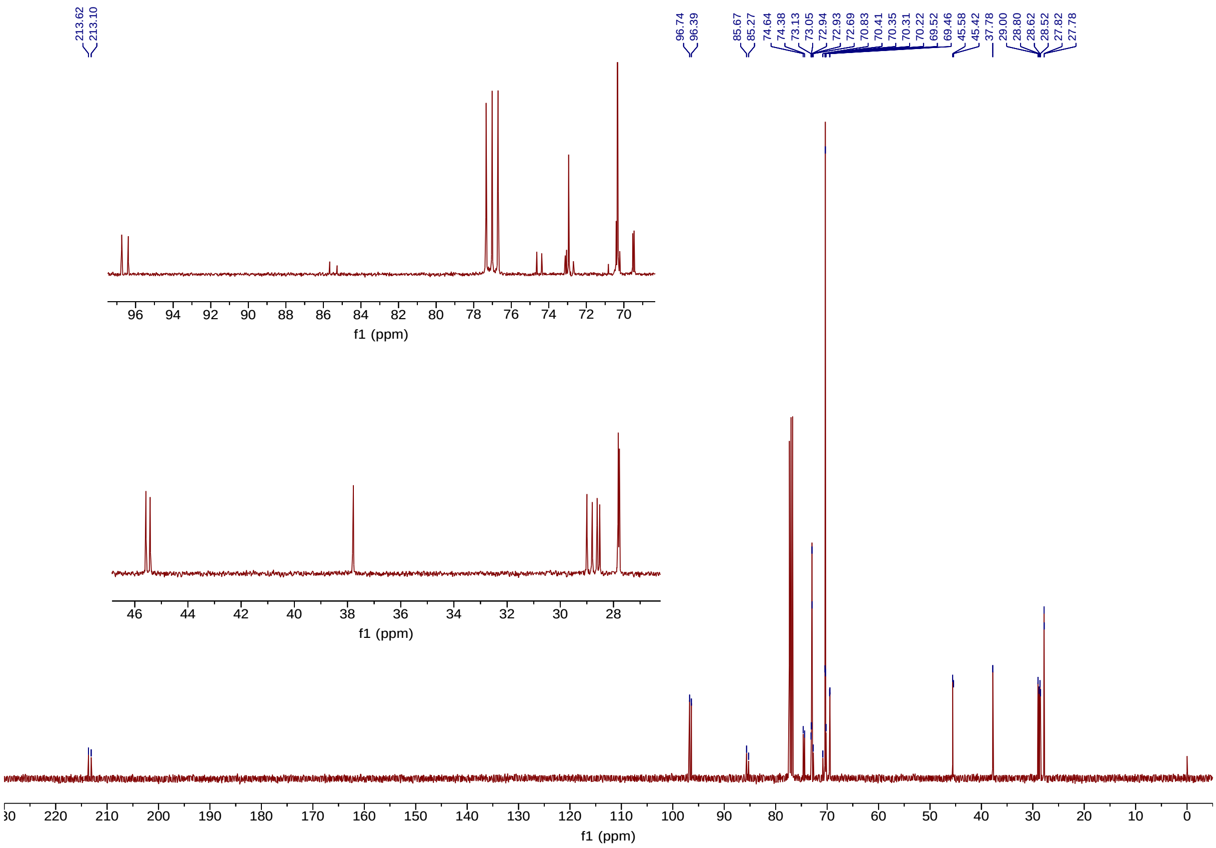

Figure S14 $^{13}C\{^{1}H\}$ NMR spectrum (101 MHz, $CDCl_3$) of **1d**

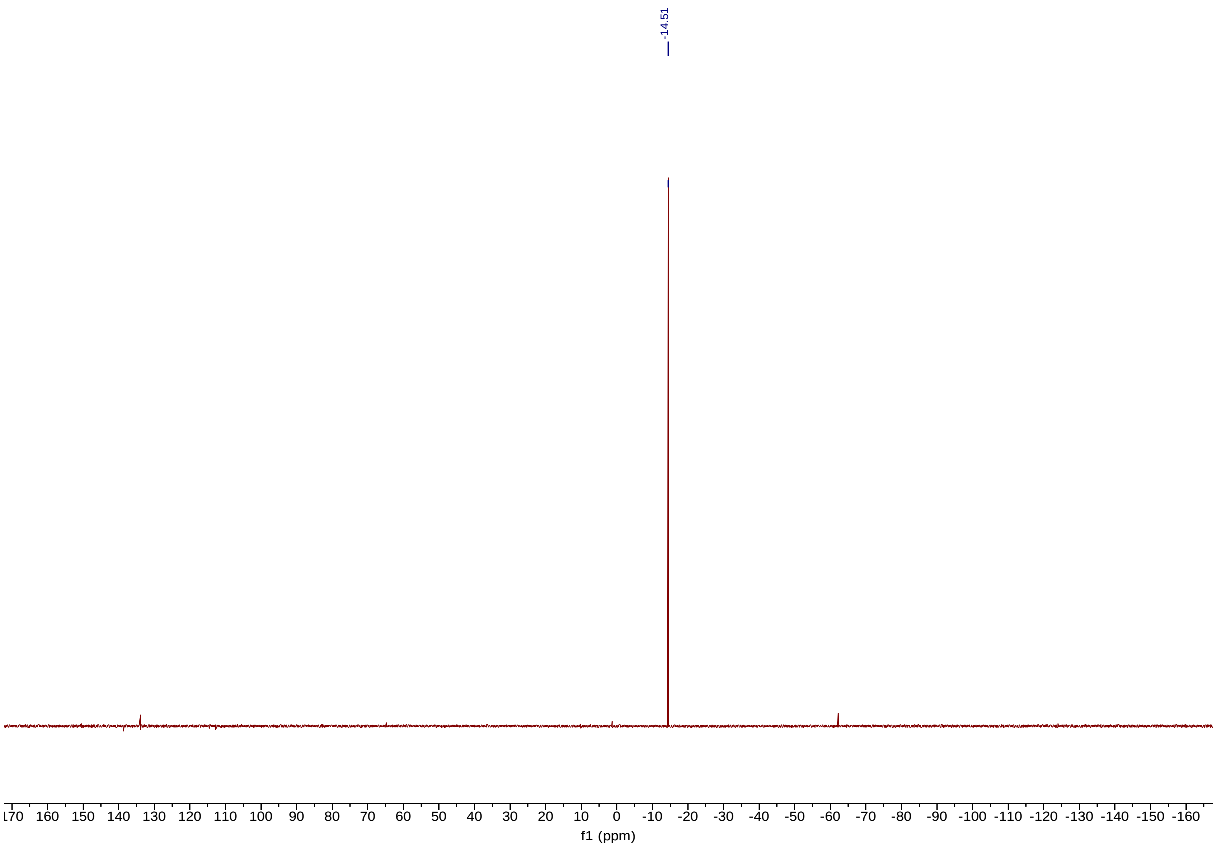

Figure S15 $^{31}P\{^{1}H\}$ NMR spectrum (162 MHz, $CDCl_3$) of **1d**

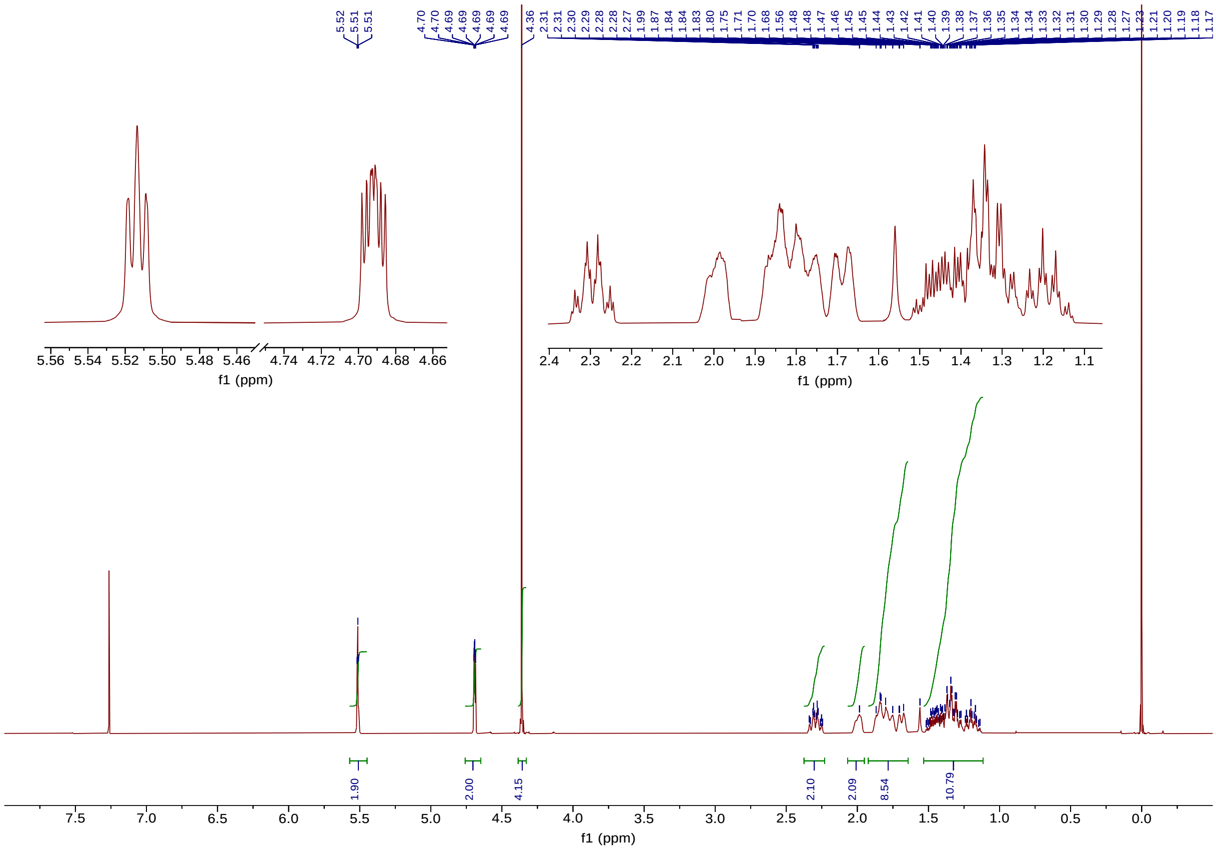

Figure S16 ^{1}H NMR spectrum (400 MHz, $CDCl_3$) of **2b**

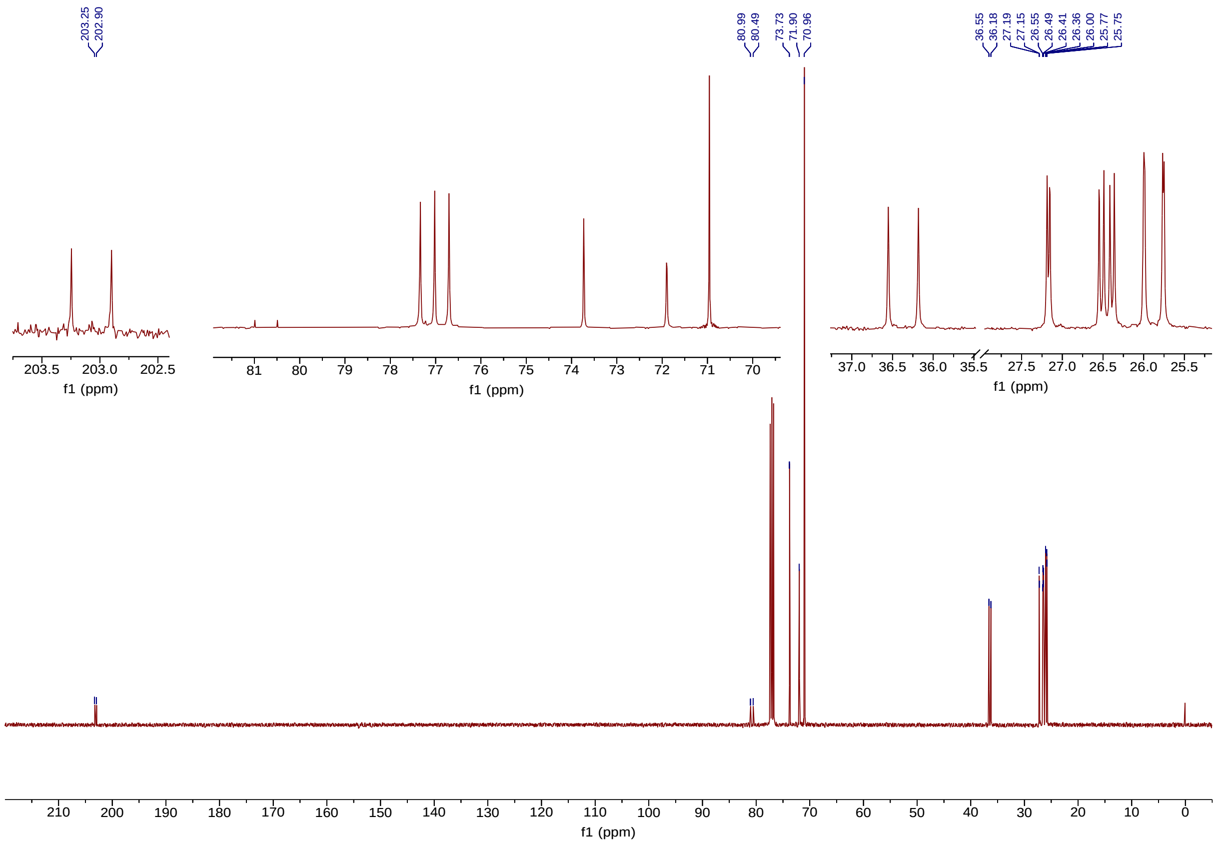

Figure S17 $^{13}C\{^{1}H\}$ NMR spectrum (101 MHz, $CDCl_3$) of **2b**

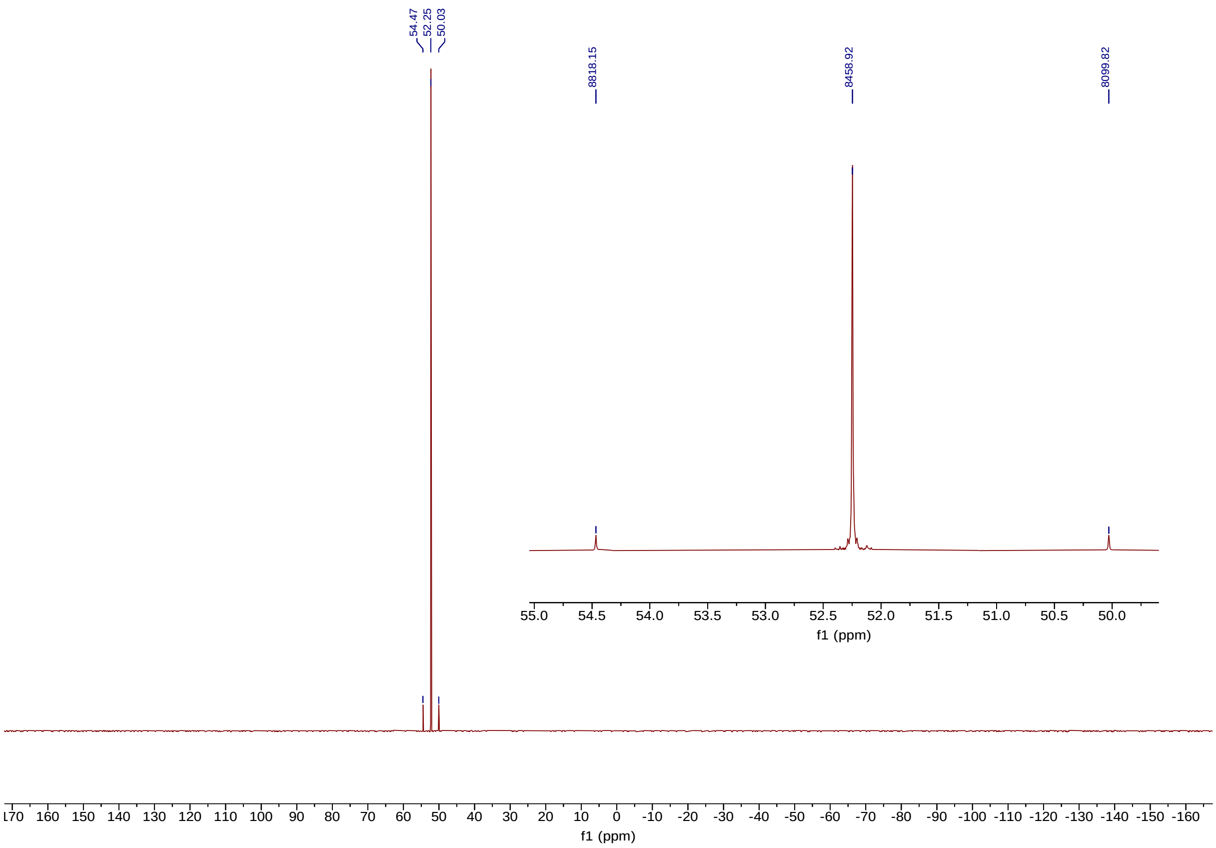

Figure S18 $^{31}P\{^1H\}$ NMR spectrum (162 MHz, $CDCl_3$) of **2b**

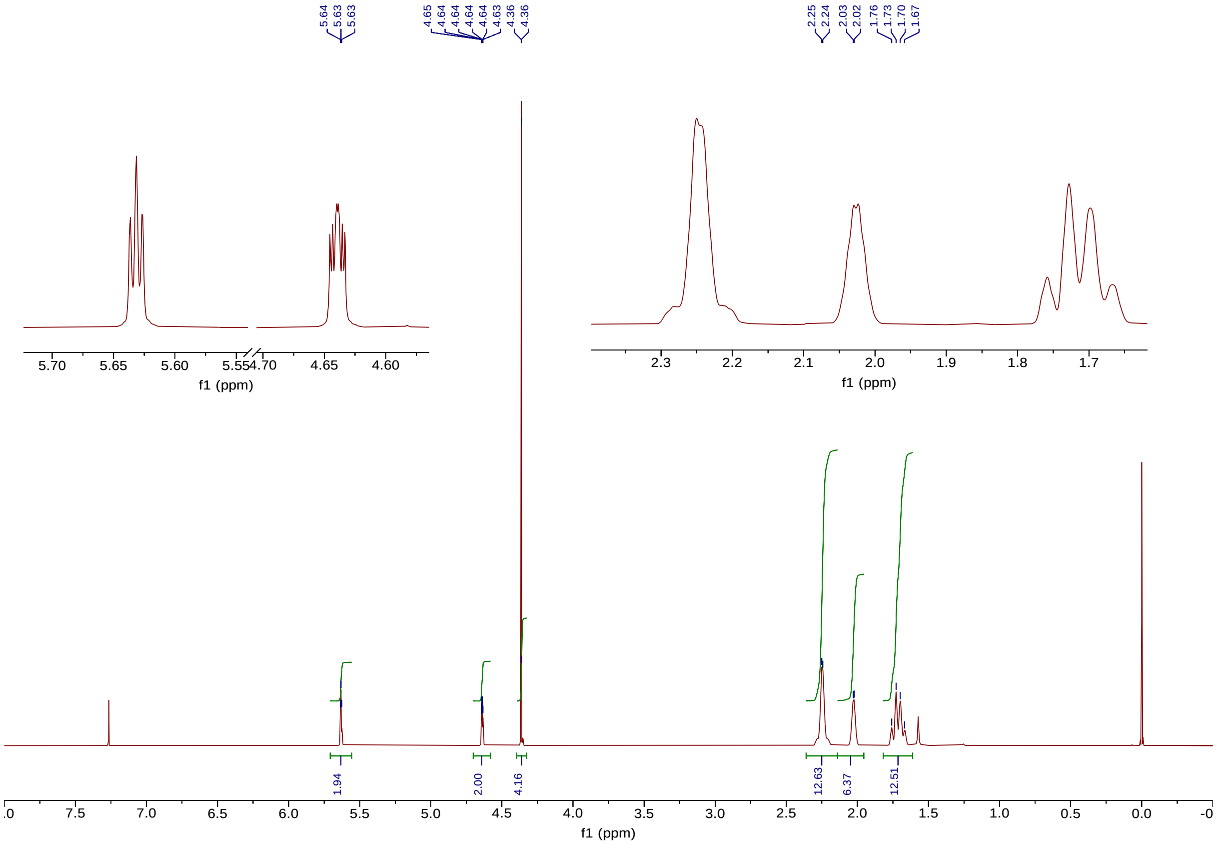

Figure S19 ^{1}H NMR spectrum (400 MHz, $CDCl_3$) of **2c**

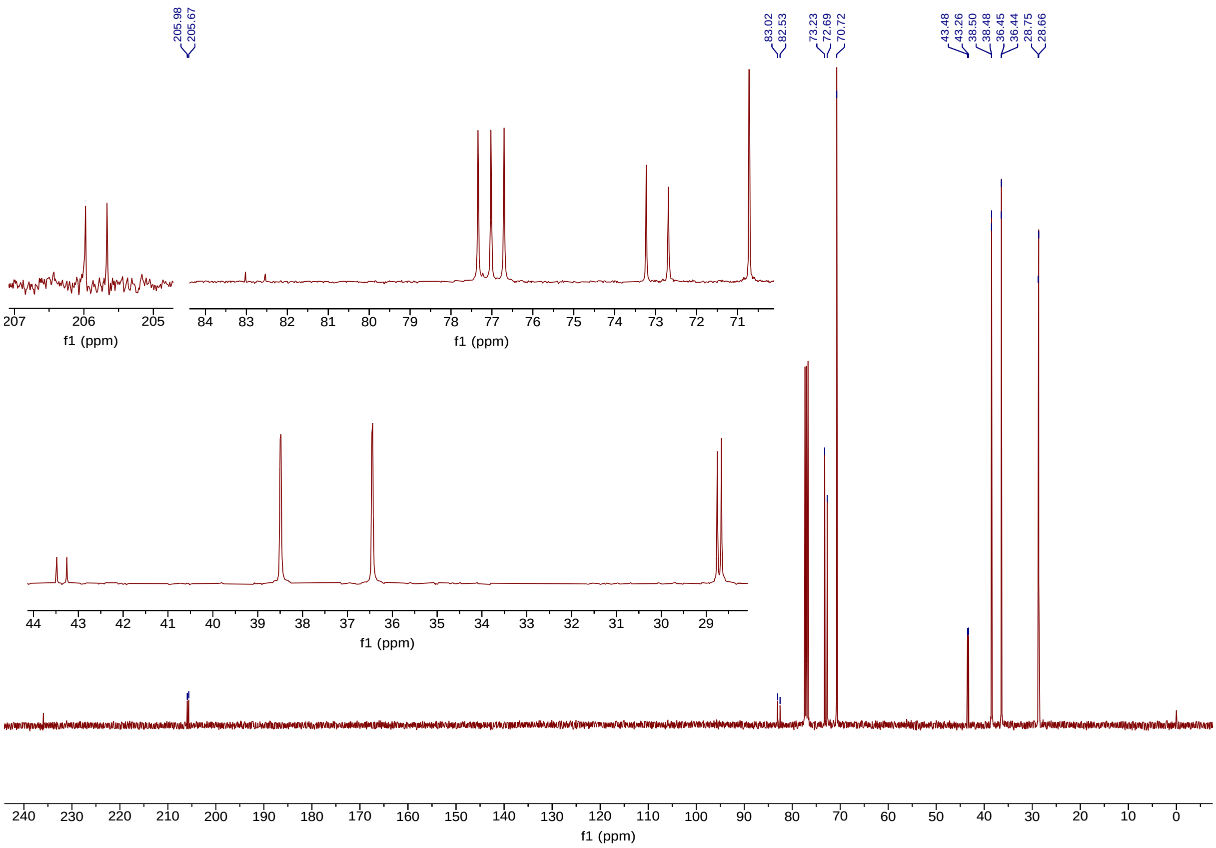

Figure S20 $^{13}C\{^1H\}$ NMR spectrum (101 MHz, $CDCl_3$) of **2c**

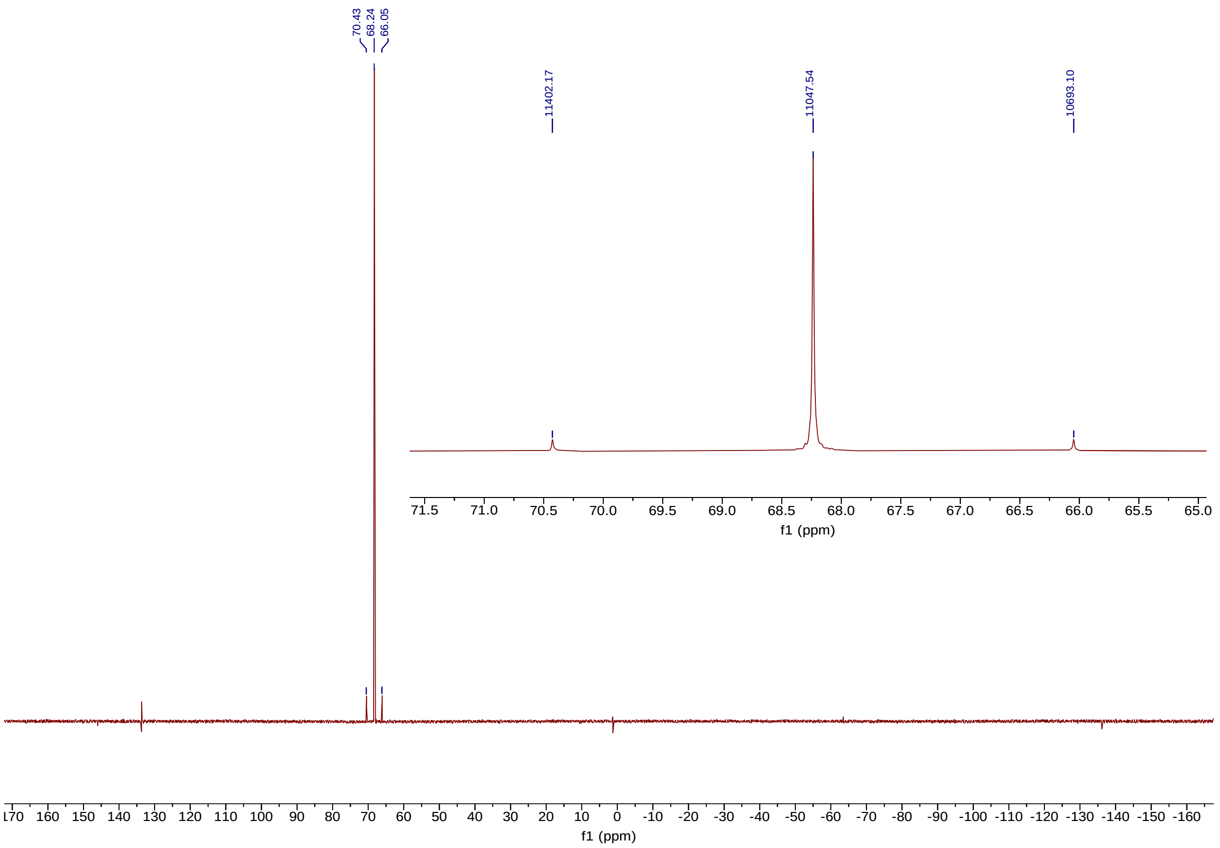

Figure S21 $^{31}P\{^{1}H\}$ NMR spectrum (162 MHz, $CDCl_3$) of **2c**

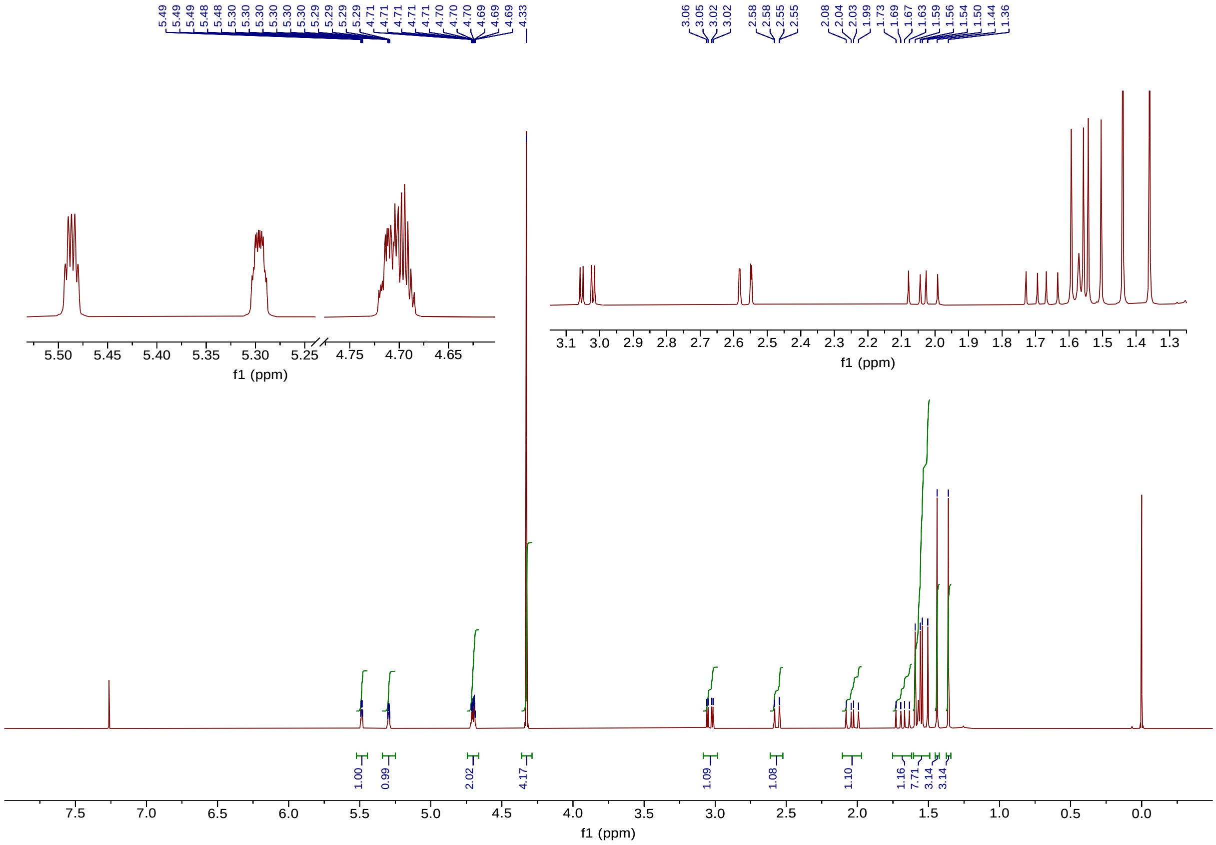

Figure S22 ^{1}H NMR spectrum (400 MHz, $CDCl_3$) of **2d**

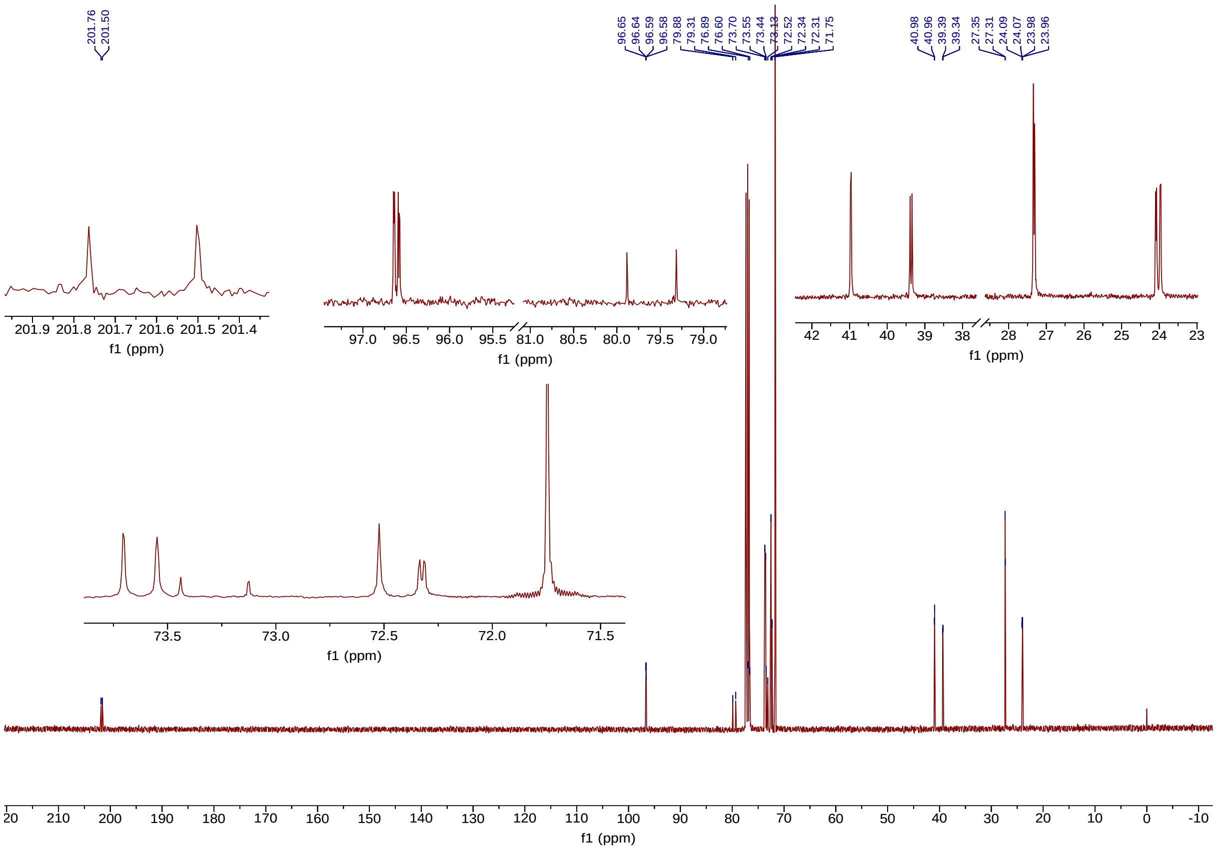

Figure S23 $^{13}C\{^{1}H\}$ NMR spectrum (101 MHz, $CDCl_3$) of **2d**

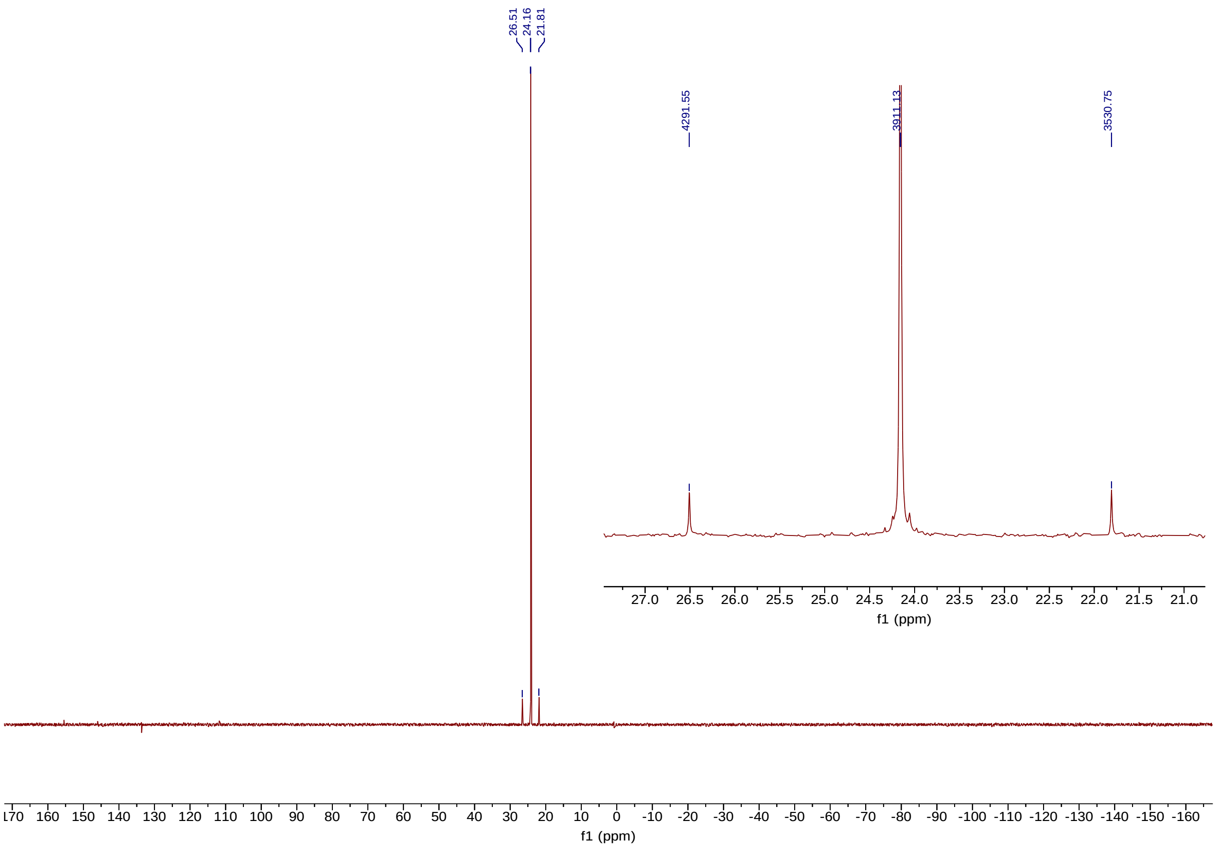

Figure S24 $^{31}P\{^{1}H\}$ NMR spectrum (162 MHz, $CDCl_3$) of **2d**

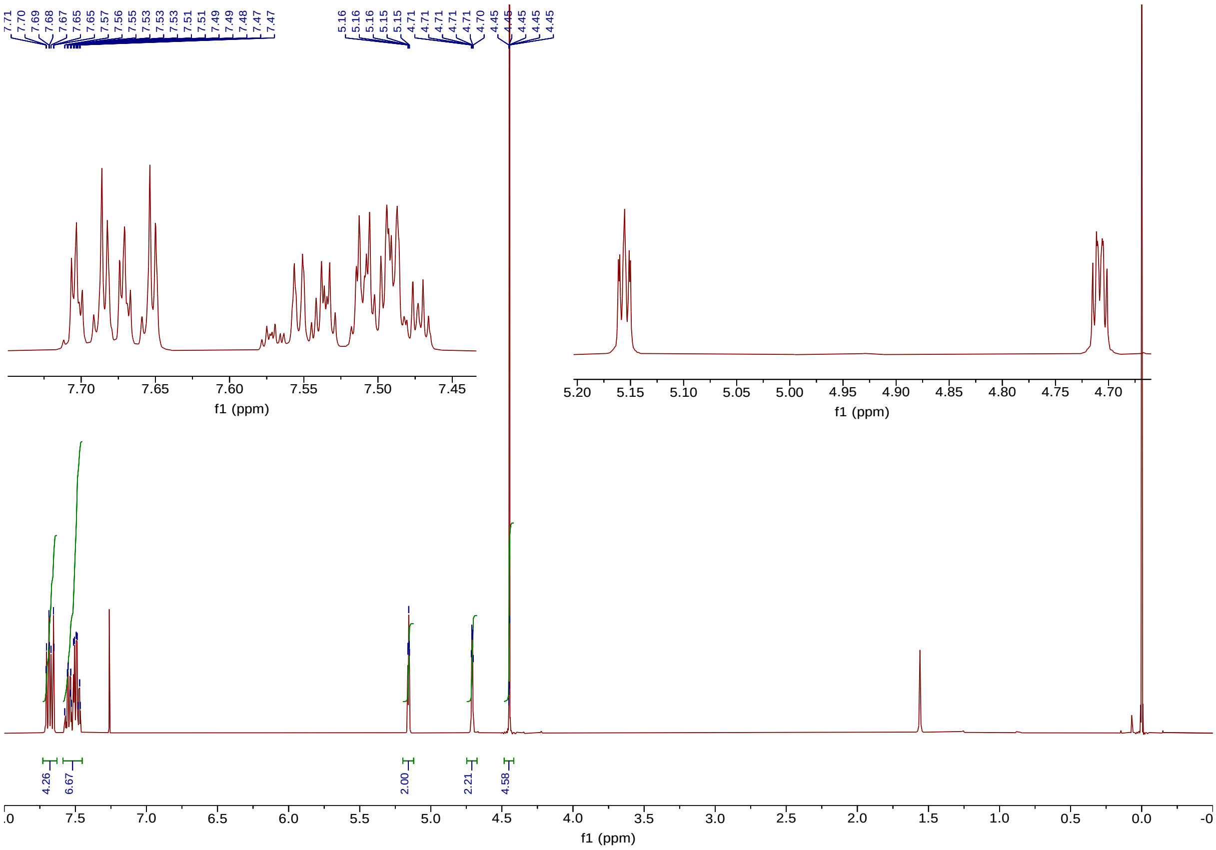

Figure S25 ^{1}H NMR spectrum (400 MHz, $CDCl_3$) of **3a**

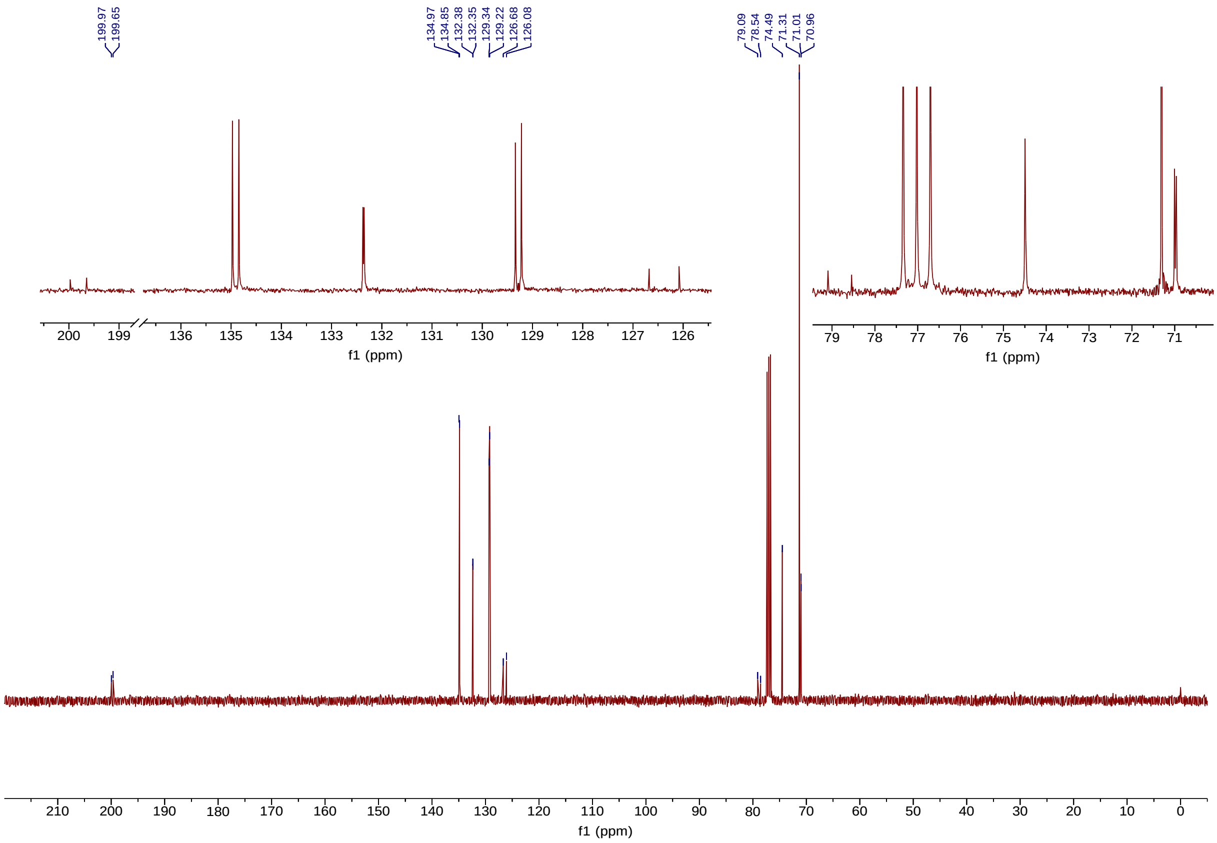

Figure S26 $^{13}C\{^1H\}$ NMR spectrum (101 MHz, $CDCl_3$) of **3a**

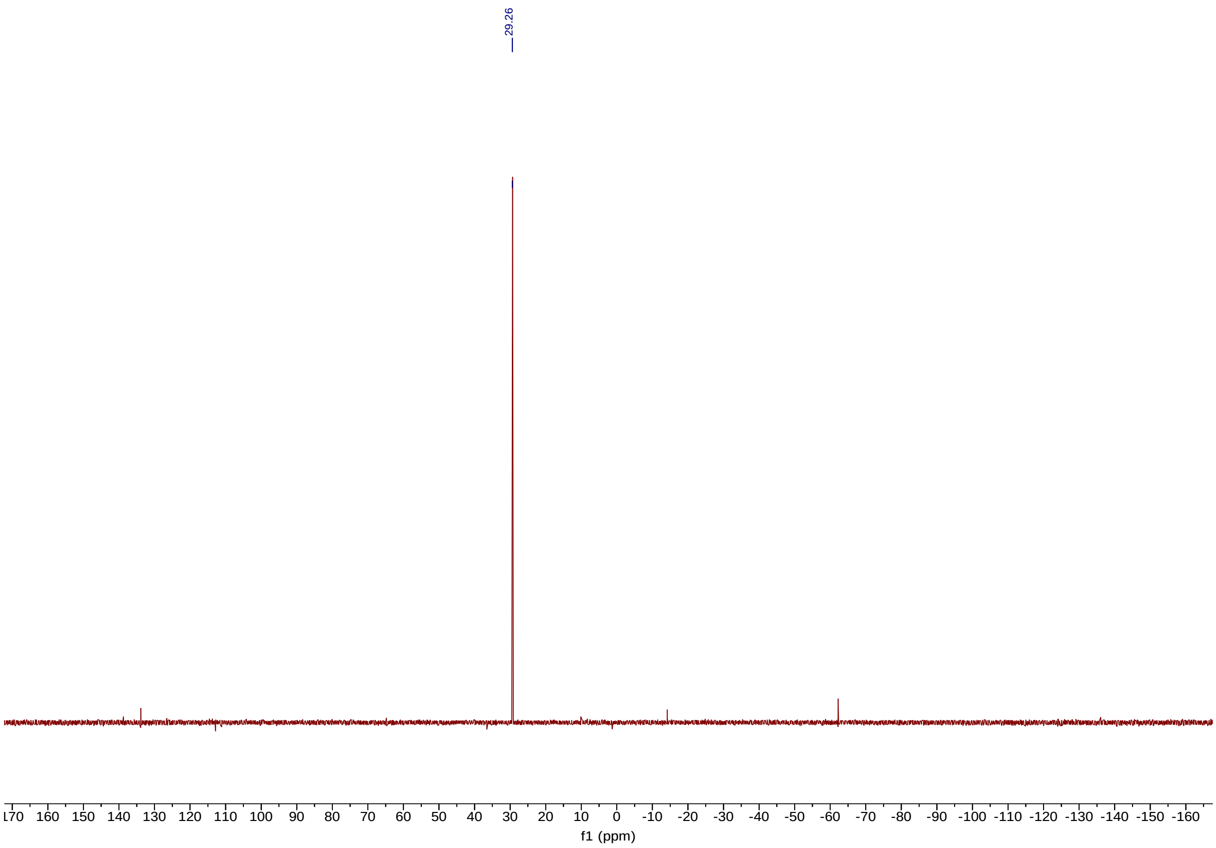

Figure S27 $^{31}P\{^{1}H\}$ NMR spectrum (162 MHz, $CDCl_3$) of **3a**

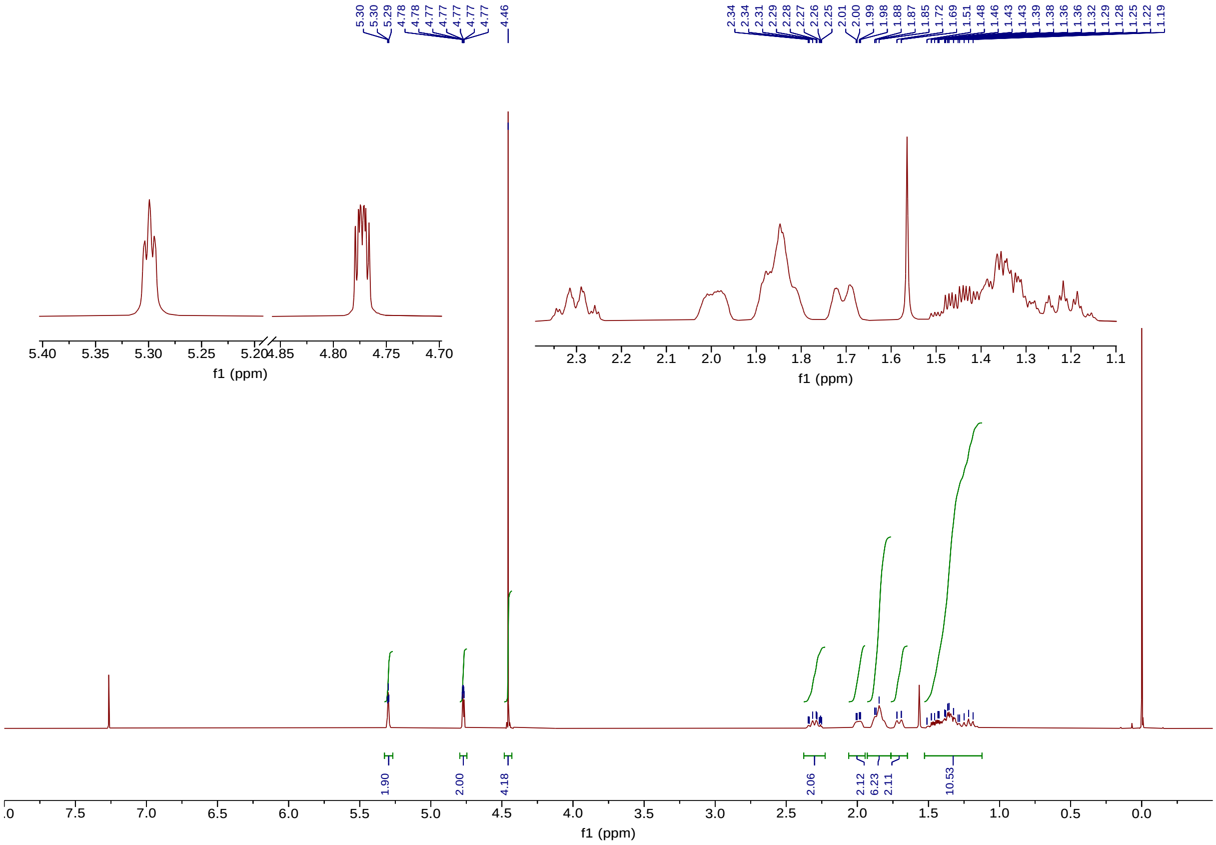

Figure S28 ^{1}H NMR spectrum (400 MHz, $CDCl_3$) of **3b**

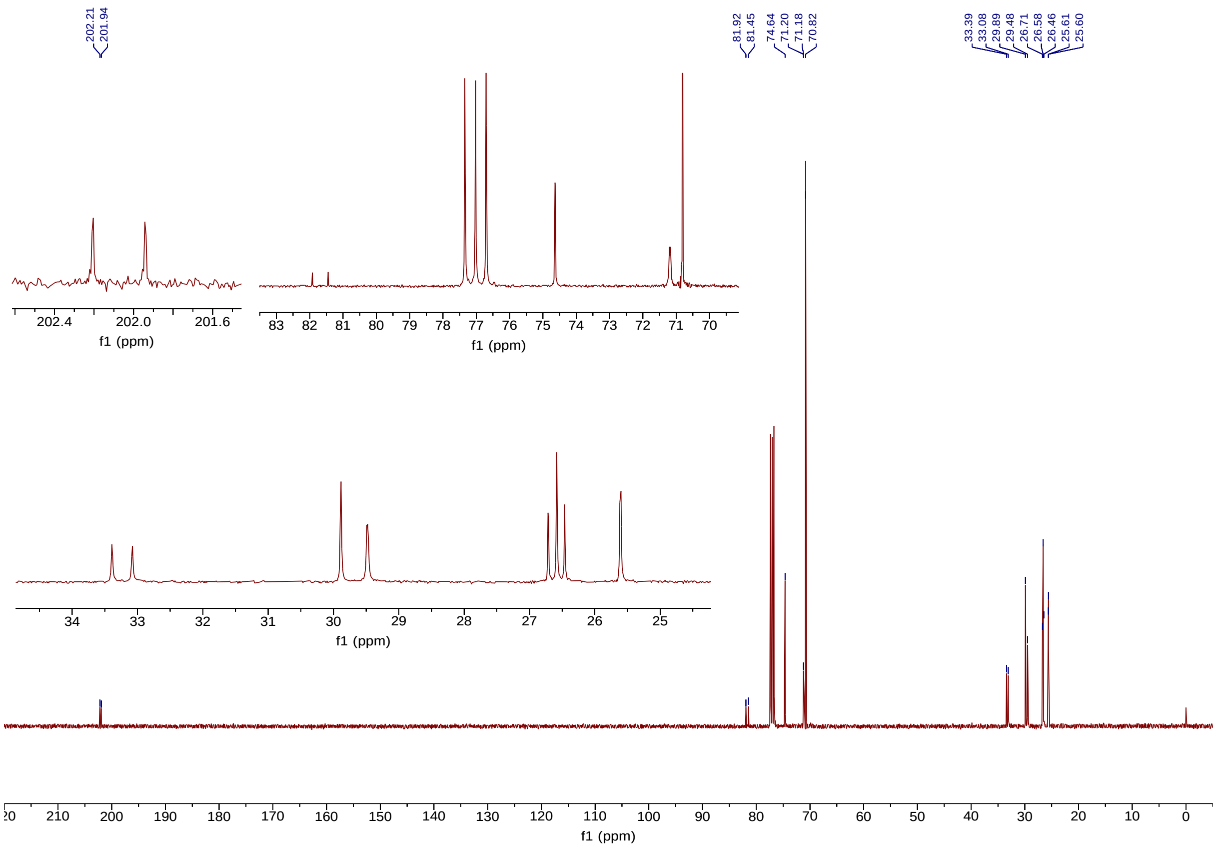

Figure S29 $^{13}C\{^{1}H\}$ NMR spectrum (101 MHz, $CDCl_3$) of **3b**

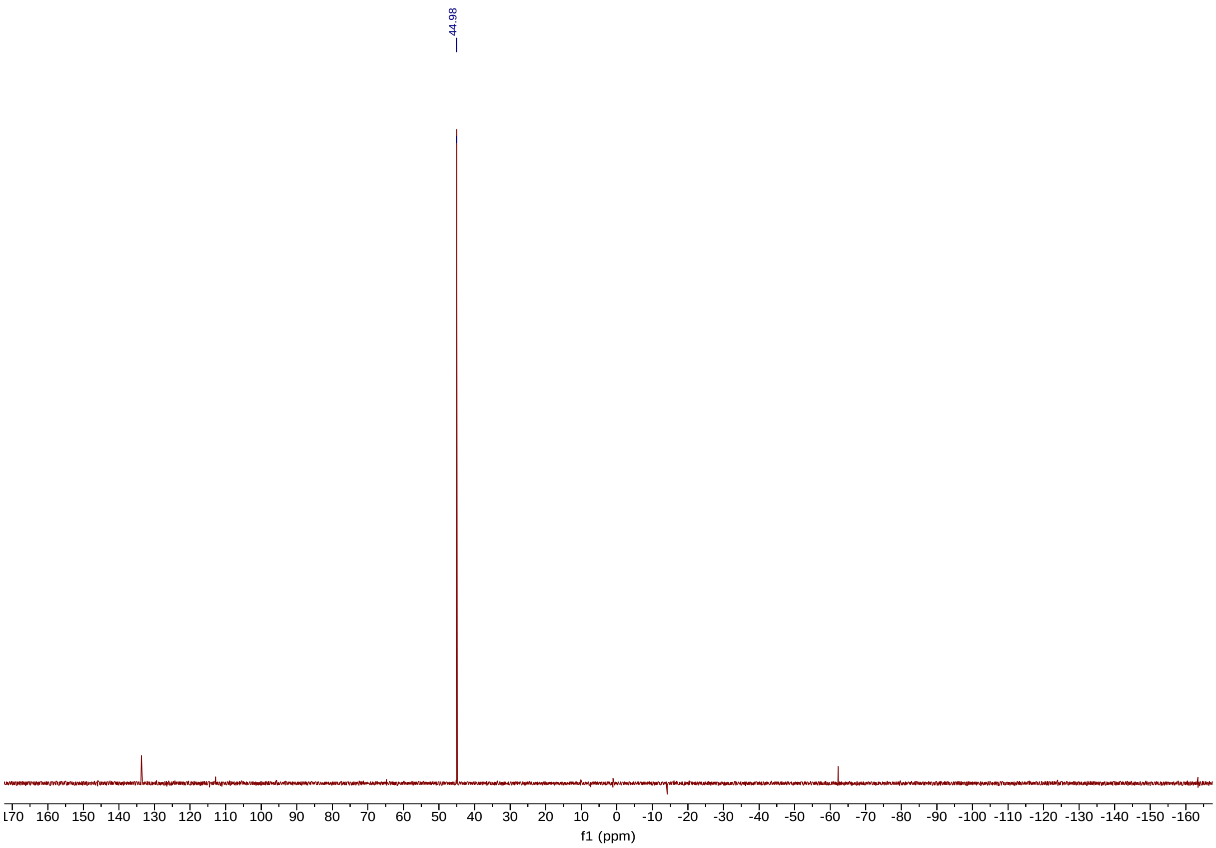

Figure S30 $^{31}P\{^{1}H\}$ NMR spectrum (162 MHz, $CDCl_3$) of **3b**

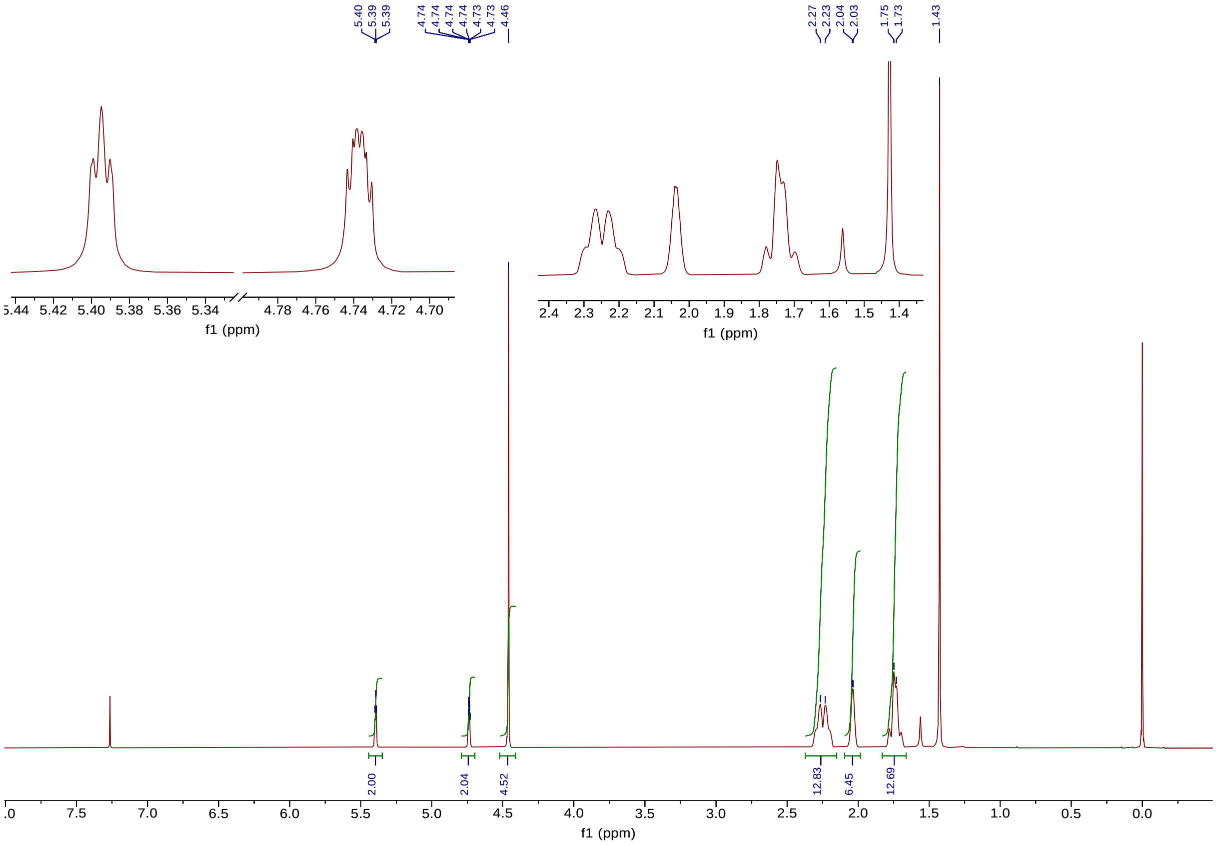

Figure S31 ^{1}H NMR spectrum (400 MHz, $CDCl_3$) of **3c**

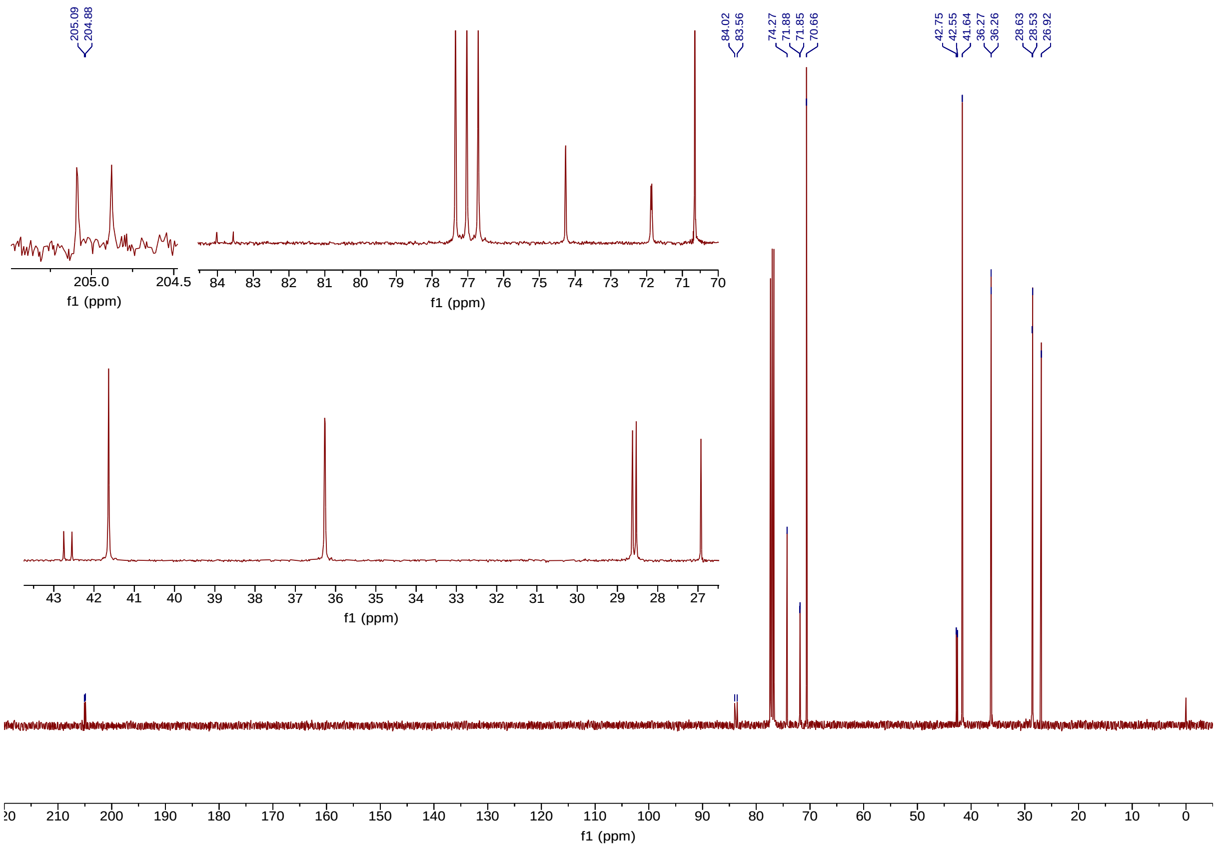

Figure S32 $^{13}C\{^{1}H\}$ NMR spectrum (101 MHz, $CDCl_3$) of **3c**

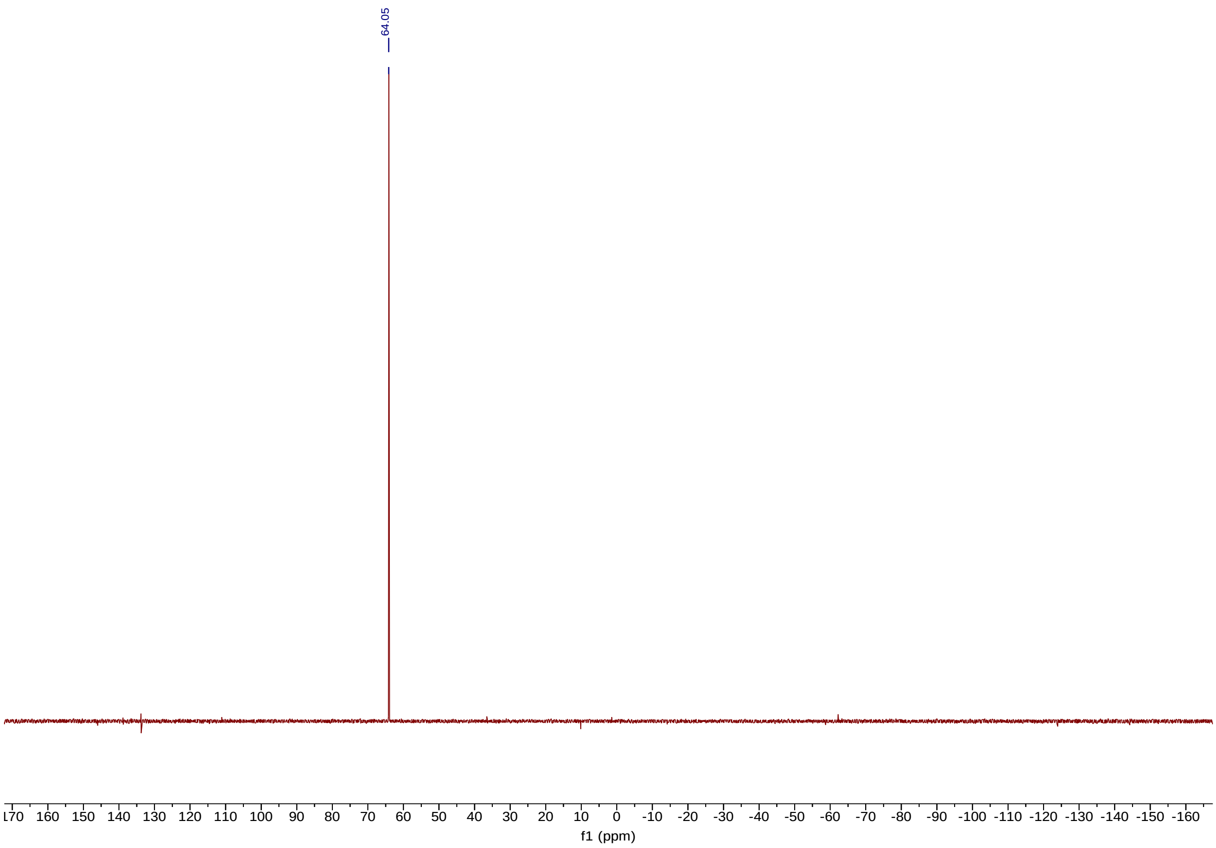

Figure S33 $^{31}P\{^{1}H\}$ NMR spectrum (162 MHz, $CDCl_3$) of **3c**

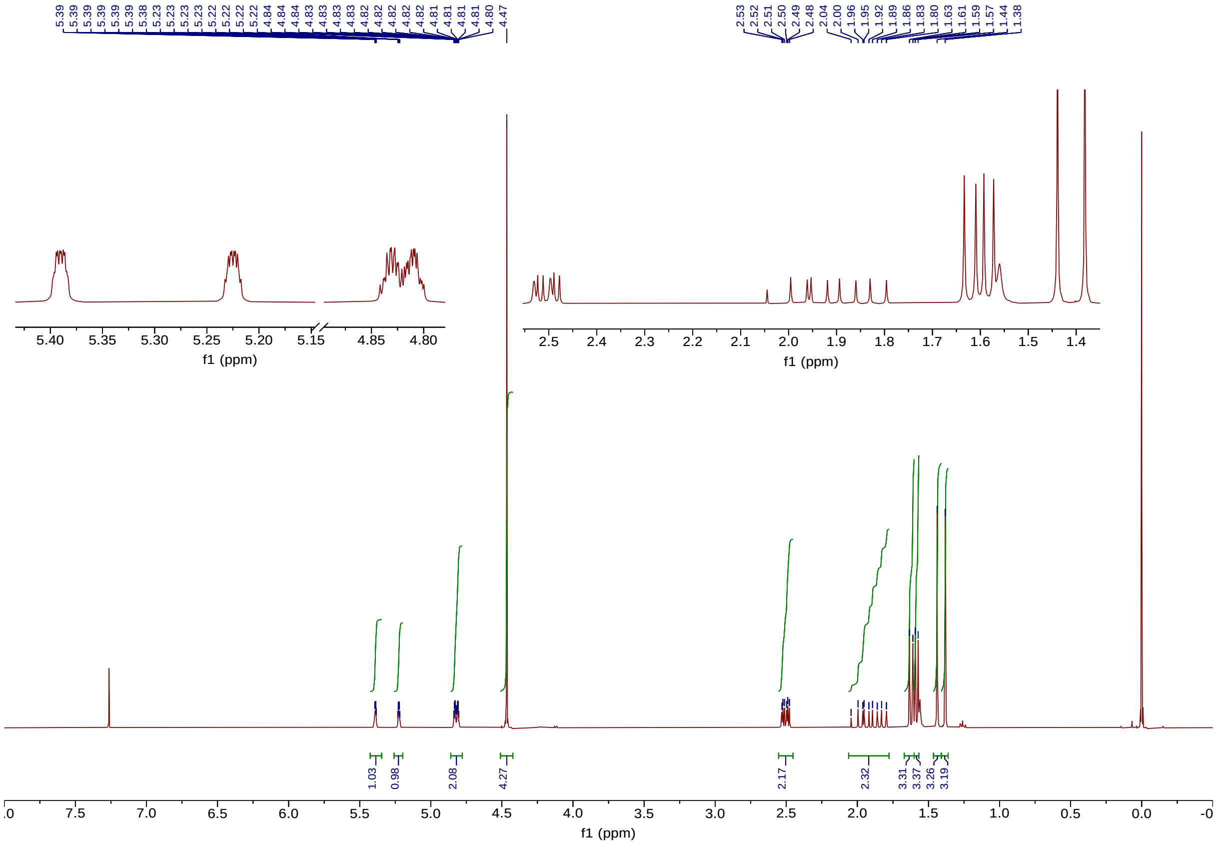

Figure S34 ^{1}H NMR spectrum (400 MHz, $CDCl_3$) of **3d**

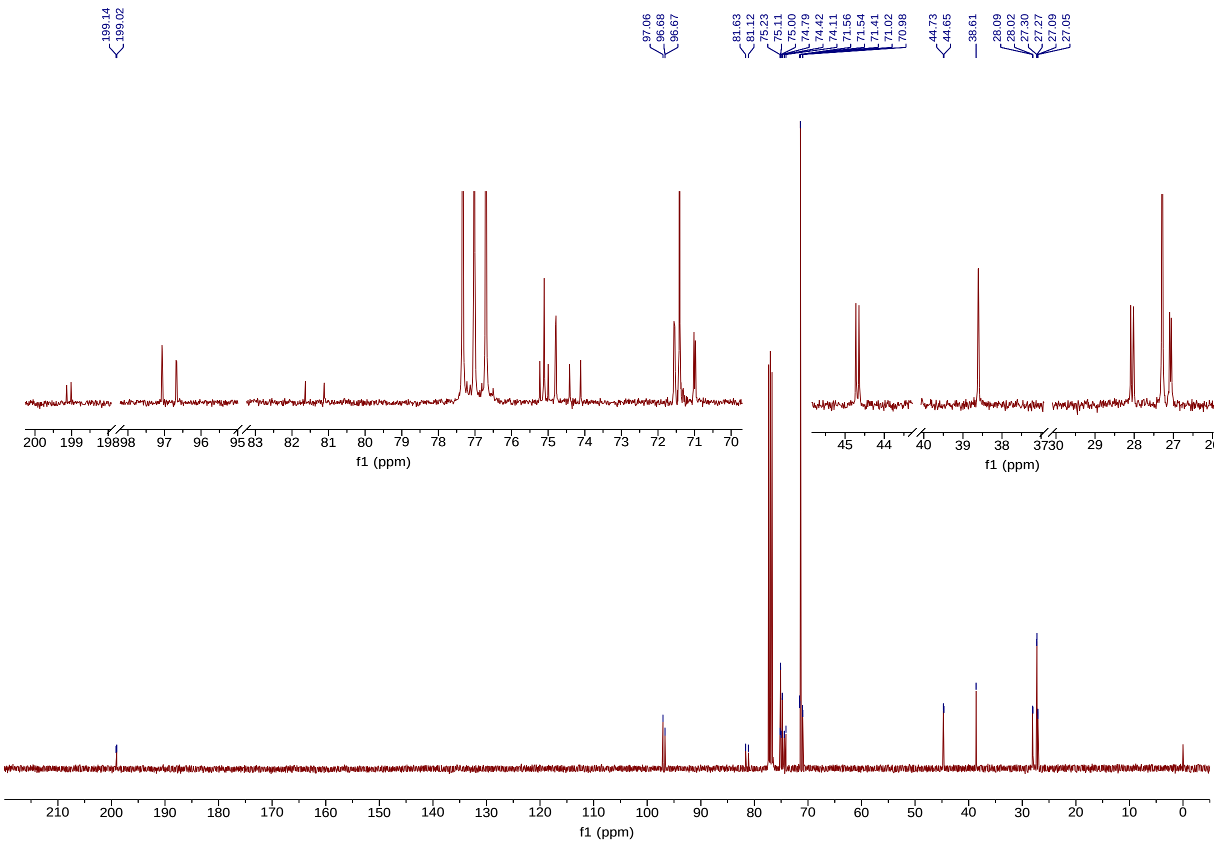

Figure S35 $^{13}C\{^{1}H\}$ NMR spectrum (101 MHz, $CDCl_3$) of **3d**

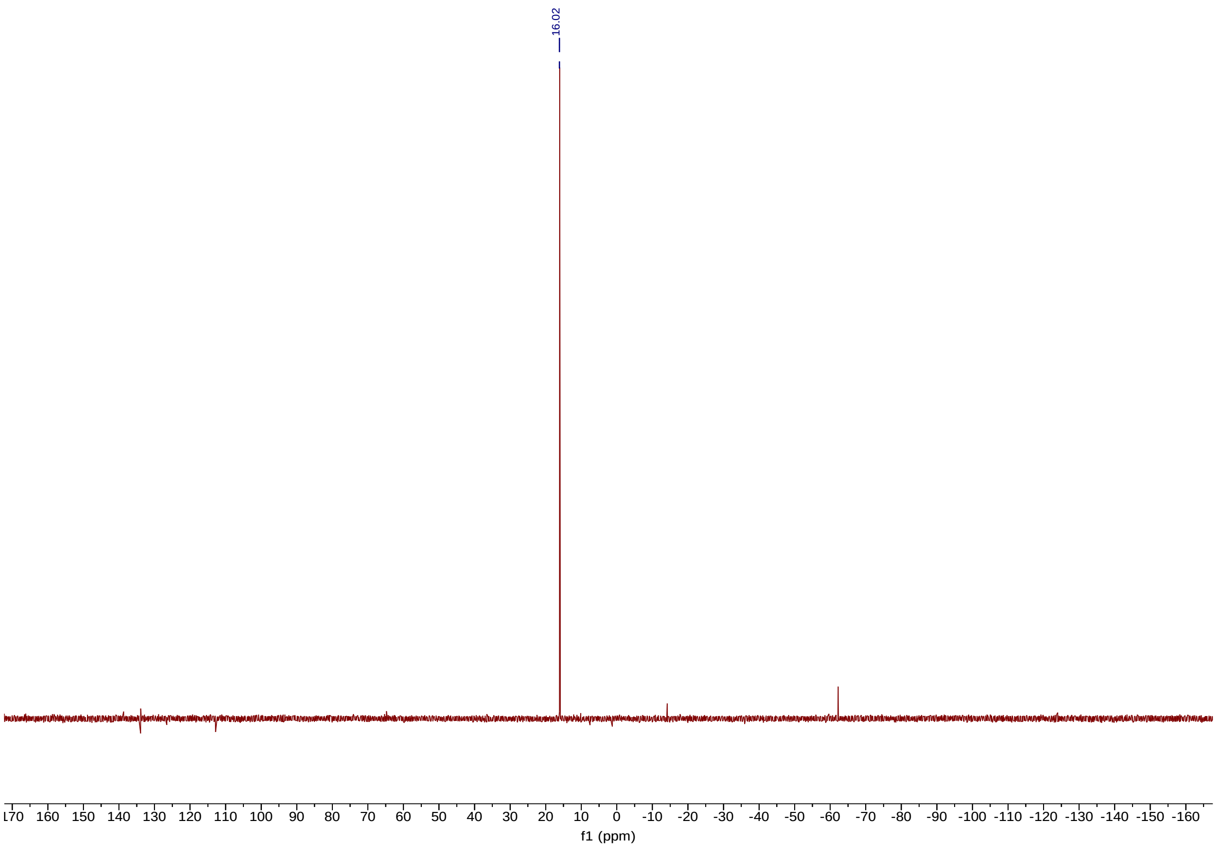

Figure S36 $^{31}P\{^{1}H\}$ NMR spectrum (162 MHz, $CDCl_3$) of **3d**

References

1 a) L. Falivene, Z. Cao, A. Petta, L. Serra, A. Poater, R. Oliva, V. Scarano and L. Cavallo, *Nat. Chem.*, 2019, **11**, 872; b) L. Falivene, R. Cudenchino, A. Poater, A. Petta, L. Serra, R. Oliva, V. Scarano and L. Cavallo, *Organometallics*, 2016, **35**, 2286.

2 A. Poater, F. Ragone, R. Mariz, R. Dorta and L. Cavallo, *Chem. Eur. J.*, 2010, **16**, 14348.